공학박사학위논문

Effect of Self-oscillation on Dynamic Characteristics of a Closed-type Swirl Injector

폐쇄형 스월 분사기에서 자체 불안정이 동특성에 미치는 영향 연구

2020년 8월

서울대학교 대학원

기계항공공학부

정 석 규

ABSTRACT

Injector is a device which can makes liquid to droplets. Injectors are used in various fields such as combustion, agriculture, cooling, etc. Injectors can be varied with atomization method, swirl-type, screw-type, impinging-type, shear-type, pintle-type, etc. Among them, owing to simple structure and high performance, closed type swirl injectors have been widely used, especially as rocket engine injector in Russia. However, when an injector is used for combustion, flow instability of injector becomes important. Combustion instability is occurred by coupling of acoustic characteristic of combustion chamber and heat release characteristics. At this time, heat release characteristics are changed with flow characteristics. If the propellant supply from the injector is incomplete or the atomization of the propellant becomes irregular, uniform heat release could not be generated. Therefore, it becomes combustion instability easy to occur. Thus, dynamic characteristics of spray flow such as periodical concentration of droplets or spray fluctuation should be investigated. Therefore, in this study, the reason of self-oscillation and characteristic of self-oscillation instability with varying experimental condition was investigated by measuring internal flow characteristic. Then, the effect of self-oscillation on swirl injector external flow was measured. Finally, the effect of self-oscillation on dynamic characteristic of swirl injector was investigated in with applying external pulsation. The result of experiments was as follows.

First, the characteristics of self-oscillation instability was found from internal flow image of swirl injector. It was found that the amplitude of self-oscillation was inversely proportional to mass flow rate and self-oscillation frequency was proportional to mass flow rate. To find the characteristics of self-oscillation frequency in more detail, experiments with various swirl injector geometry was

done. As a result, it was found that amplitude of self-oscillation was related to liquid momentum. On the other hands, it was found that frequency of self-oscillation was related to liquid axial velocity at the orifice. This phenomenon was same as Kelvin Helmholtz instability. Relation of frequency and velocity could be represented from Strouhal number, and in this study, constant Strouhal number, 0.236 was found in all experiment cases.

Second, the effect of self-oscillation on swirl injector flow was investigated. It was found that the phenomenon of instability at external spray angle and internal air core diameter was same. The effect of the self-oscillation on external spray then investigated in more detail. At first, wave characteristic with sheet propagation was investigated from spray images. Self-oscillation frequency remained same with spray flow progression, and fluctuation amplitude was only increased. Effect of self-oscillation on breakup process was then examined. In this time, breakup occurred periodically, which have period same as inverse of self-oscillation frequency. Moreover, spending time between sheet progress and droplet conversion was different. Due to this difference, periodical concentration of droplet flow was formed.

Finally, the effect of external pulsation on swirl injector flow and the relation between injector dynamic characteristic and self-oscillation was investigated. At this time, specific frequency could be applied at the feed line by using the hydraulic mechanical pulsator. Experimental condition which had 312 Hz self-oscillation frequency was used for this investigation. Dynamic gain was measured from air core diameter with respect to frequency, and the maximum gain found at the frequency same as self-oscillation frequency. Breakup length with respect to excitation frequency was then measured. Breakup length was minimum at the frequency same as self-oscillation frequency due to the high wave fluctuation. From the result, the fluctuation amplitude and breakup length were determined to be inversely related, and self-oscillation frequency was inferred to have some role on the dynamic characteristic of breakup length. Both the mean drop size and the

SMD were smaller than those without pulsation. In addition, when the pulsation was performed at the injector self-oscillation frequency, an unusual phenomenon occurred for the SMD. The SMD was confirmed to become larger when excitation was performed at the injector self-instability frequency. This tendency seems to be due to the non-uniform distribution of droplets in the case of self-instability frequency pulsation.

In conclusion, through this study, experimental data on the self-oscillation instability phenomenon of a single liquid swirl injector were obtained. Furthermore, the manifestation of unstable spray characteristics, when nonlinear large pulsation was applied, was experimentally confirmed. Self-oscillation with external pulsation was also confirmed to possibly change the characteristics of injector, especially breakup length and SMD, which is a combustion-related factor. Therefore, knowledge of self-oscillation frequency of injector is important for engine system design. Furthermore, frequency of pressure noise from feed system should be confirmed before entire engine system combining to prevent engine failure. Additionally, further research may be needed to clarify the relationship between self-instability, SMD, and combustion through an actual combustion test in the presence of such an instability.

Keywords: Closed-type Swirl Injector, Flow Instability, Injector Self-oscillation Instability, Injector Dynamics, Mechanical Pulsator, Kelvin-Helmholtz Instability

Student Number: 2014-21891

LIST

LIST OF FIGURES

LIST OF TABLES

NOMENCLATURE

Alphabet

FFT	Fast Fourier Transform
RMS	Root Mean Square
SMD	Sauter Mean Diameter
A	area, mm^2
C	angular momentum constant, m^2/s
D	diameter, mm
D_H	hydraulic diameter, mm
D_{10}	Mean droplet size
f	Total growth of wave = $\ln(T/T_0)$
f_s	Self-exctied instability frequency of injector
f_e	Frequency of external pulsation
K	injector geometric constant
k	wave number
L	length, mm
$\dot{m}$	mass flow rate, g/s
N_t	number of tangential inlets
P_m	Pressure drop through the injector
R	inflow radius, mm
T	Wave fluctuation amplitude
T_0	Initial wave fluctuation amplitude
U	flow velocity, m/s
x	Distance of sheet in flow direction
y	Displacement of wavy sheet at a distance x
α	reflection coefficient
α_c	swirl chamber converging angle, degrees
ε	orificve filling coefficient

θ	spray half angle, degrees
θ_p	Phase angle
ξ	wave position, mm
ρ	water density, kg/m^3
Ω	surface wave amplitude
ω	angular disturbance frequency with stationary condition

Subscript

a	air core
ax	axial
b	breakup
in	injector inlet
o	orifice
t	tangential inlet port
tan	tangential
s	swirl chamber

CHAPTER 1

INTRODUCTION

A typical combustion engine consists of injector, combustion chamber, and nozzle. In the engine, the propellant is burned after the atomization, vaporization, and mixing processes to generate energy, and an injector is a device that spray propellant into the combustion chamber, which is an essential element for stable combustion in the combustion chamber. There have been various types of injectors depending on the atomization method. Among them, the swirl injector has a stable and high atomization performance despite its simple structure. Therefore, swirl injectors have been widely used for combustion engine, including Russian rocket engines.

Figure 1 shows general geometry of a liquid single swirl injector. Atomization principle of swirl injector is as follows. Initially, liquid in the manifold enters the swirl chamber through the tangential inlet. Since inlet ports are connected to the tangential direction of the swirl chamber, the liquid flow flows along the surface wall while rotating in the swirl chamber and proceeds to the outlet with tangential velocity. After flow leaves the injector wall, it is spread by centrifugal force and form a spray with thin liquid sheet. As the flow continues, the liquid film becomes thinner. As a result, no longer retains the liquid film and splits into droplets. Depending on the absence or presence of converging section at the swirl chamber, swirl injector is

divided into an open type and a closed type. Normally, closed type swirl injector has high performance due to high angular momentum at the end of the orifice due to the velocity acceleration through the converging section.

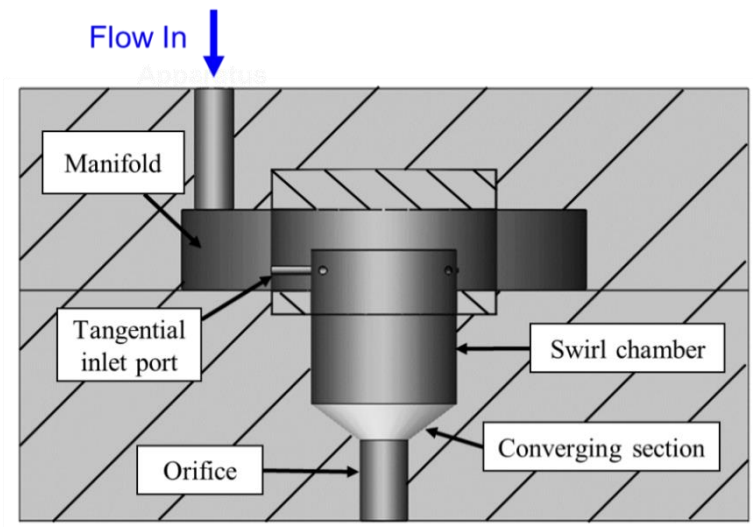

Fig. 1.1 Scheme of closed-type swirl injector

When an injector is used for rocket engine, flow instability characteristics of an injector become important due to the relation with combustion instability. The combustion instability of an engine is a phenomenon in which the pressure fluctuation inside the combustion chamber increases due to the coupling of the heat release perturbation and the acoustic characteristics of the combustion chamber structure. When combustion instability occurs, it can cause not only reduction of the combustion efficiency, but also engine failure in serious cases. In rocket engines, baffles or acoustic cavities are mainly used to suppress combustion instability. However, because additional parts should be installed in the engine, baffles or

acoustic cavities reduce engine efficiency. On the other hand, by changing injector characteristics, combustion instability can be suppressed without additional parts in the engine. By controlling the flow characteristics through changes in the injector geometry, it is possible to suppress instability by changing the heat release characteristics which affect combustion instability.

In general, the propulsion system consists of three parts: feedline, injector, and combustion chamber. A schematic of the dynamic process of the system is shown in Fig. 1.2 (Bazarov, 1979, Bazarov and Yang, 1998). When the pressure perturbation occurs during the combustion process, it affects the combustion chamber itself. This chamber pressure fluctuation could also affect fluctuation of injector differential pressure, which could produce velocity fluctuation at the injector. The generated velocity perturbation at the injector affects the pressure fluctuation at the feed system. Because propellant flows from feed system to injector, pressure fluctuation at the feed system influences the velocity perturbation of the injector. That is, the fluctuation at any propulsion system could affect all the system. If the perturbation of the entire system operates with positive feedback, the instability gradually increases, thereby causing engine failure. At this time, as the injector serves as an intermediate bridge for the entire propulsion system, it is possible to control the entire combustion instability by changing the injector based on a suitable design. In order to adjust the characteristics of this injector, it is important to accurately understand the dynamic characteristics of the injector. These studies are called injector dynamics, and several studies have been conducted in various groups.

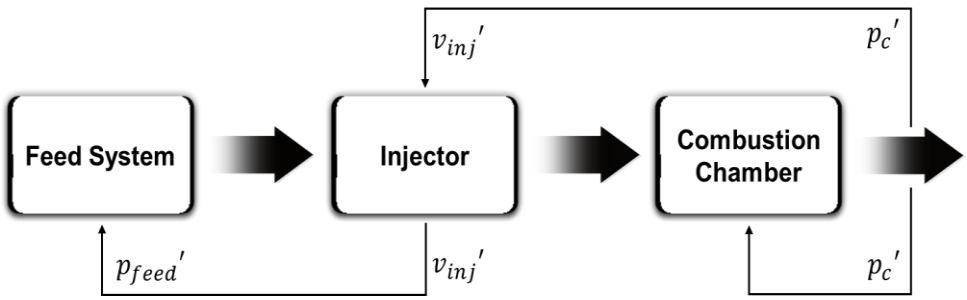

Fig. 1.2 Scheme of dynamic process interaction in the propulsion system

Injector dynamic studies were focused not only on the static characteristics such as the spray angle and liquid film thickness of an injector, but also on its dynamic characteristics to investigated relation between injector and combustion instability. Bazarov (1979) established the injector dynamics theory and defined the injector transfer function as the output divided by the input pressure. The gain of injector transfer function could provide instability amplitude and the phase of injector transfer function could provide whether an injector becomes stable or unstable. Ismailov et al. (2011a, 2011b) theoretically and numerically studied the flow instability caused by the surface wave generated inside a closed-type swirl injector. They found that swirl chamber geometry, especially length of injector head to converging section and angle of converging section, was largely related on flow instability which occurred by resonance of surface wave in the swirl injector. Chen et al. (2014) numerically analyzed the flow characteristics of a swirl injector according to the changes in the atmospheric pressure conditions, and analyzed the unstable phenomenon occurring inside the injector. Some groups carried out experimental studies on the internal flow characteristics of a swirl injector using a

high-speed backlight imaging technique to confirm dynamic characteristics at the air core (Kim, S. et al, 2008, Kenny, R. J. et al, 2009). However, these studies mainly focused on the instability response of the injector due to excitation from the injector geometrical factors, and only few studies have been conducted on the dynamic characteristic of instability that occurred in the injector itself.

In the swirl injector, there are some oscillators which can make the flow self-unstable. Some representative fluid oscillators are shown in Fig. 1.3 (Eberhalt and Frederick, Jr, 2017). First, acoustic instability could be occurred at air core in the swirl chamber. According to length and volume of air core, fundamental acoustic waves could be generated at the air core. It could produce acoustic instability with specific frequency and give effect on the liquid sheet flow in the injector. Next, hydraulic characteristic of liquid could occur self-instability. Generally, hydraulic instability of feed line or wave characteristic in the swirl chamber owing to geometry of injector contains of hydraulic instability. Injector dynamics mainly focused on this type of instability. Finally, shear layer instability at the boundary of liquid and gas could generate wave type instability. Due to the velocity difference at the liquid and gas intersection, frictional force could be generated at the shear layer. This kind of instability also called Kelvin-Helmholtz instability.

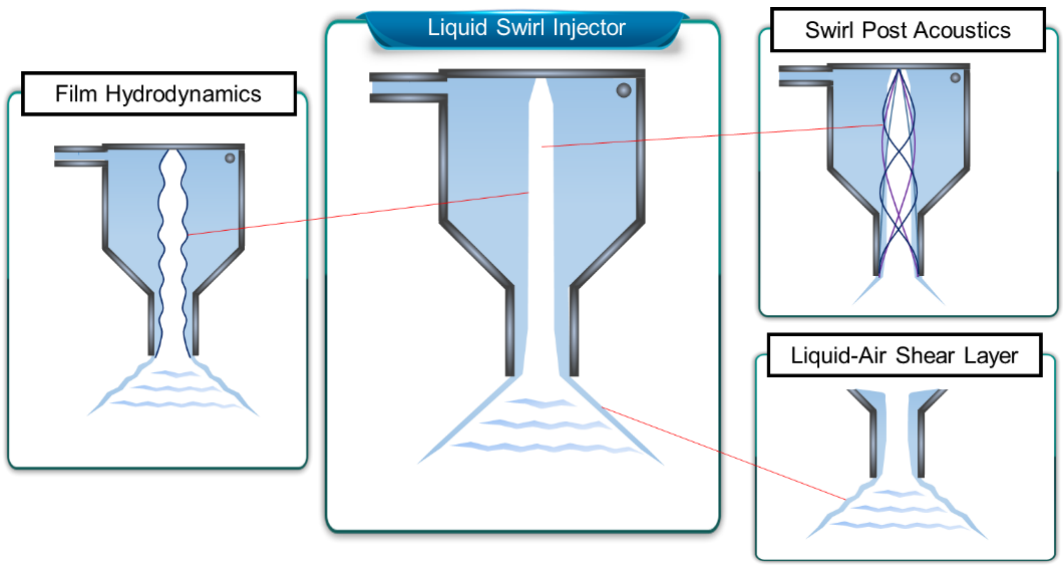

Fig. 1.3 Fluid oscillators of swirl injector element

Self-unstable flow characteristics of injectors have been developed from studies of instability in thin liquid films. Thin liquid film often develops in the form of waves affected by external aerodynamic force, and the most optimum wavelength can be theoretically calculated (Squire, 1953, Dombrowski and Johns, 1963). Based on these basic principles, methods of predicting characteristics of thin liquid sheet flow have been studied. Theories for predicting thin liquid sheet breakup process were largely composed of linear and non-linear models (Dasgupta, 2019). Linear models suggest that the most optimum wave number can be determined from the maximum growth rate. As simplified model, plane sheet was investigated theoretically and experimentally (Squire, 1953, Dombrowski and Johns, 1963). Next, Panchagnula et al. (1996) investigated annular liquid sheet with swirling flow by considering

tangential velocity term. Liao et al. (1999) found linear characteristic of swirl atomizer by considering tangential velocity component. Also, they used CFD methods to found more accurate characteristics. However, wave amplitude could be greatly enlarged with sheet moving. Thus, linear assumption, which assume that amplitude of disturbance is small, alone has a limit in predicting actual breakup time and breakup length. Accordingly, research on non-linear instability has been conducted. It makes possible to predict more accurate breakup length and breakup time. Rangel and Sirignano (1991) investigated instability characteristic of wavy fluid sheet using linear and nonlinear calculation. Jayareri and Li (2000) investigated breakup characteristic of plane liquid sheets including third order term at governing equation to get more accurate characteristics. For swirl injector flow, Chen and Yang (2014) numerically investigated flow dynamics of closed-type liquid swirl injector and Kang et al. (2018) experimentally found the relation between wave characteristic and film velocity by using POD analysis. However, these studies mainly focused on the prediction of breakup due to instability, rather than on the frequency characteristic which is important in combustion instability.

Swirl injector could have unstable spray characteristics depending on the structure and conditions, even though injectors have similar flow rates. If the flow is unstable, it is hard to produce stable combustion. However, effect of self-instability on static and dynamic characteristic of swirl injector have not been dealt in depth. Especially, experimental studies were insufficient to find the effect of self-instability on flow characteristic. Therefore, in this study, the self-instability phenomenon of

the swirl injector was experimentally performed from the viewpoint of dynamic characteristics. In Chapter 3, the reason of self-oscillation instability and characteristic of self-oscillation with varying experimental condition was investigated by measuring internal and external flow characteristic. Then, the effect of self-oscillation on swirl injector external flow was measured in Chapter 4. Finally, the effect of self-oscillation on dynamic characteristic of swirl injector was investigated in Chapter 5 with applying external pulsation. With these procedures, the importance of self-instability characteristics in the injector used for combustion and the design method considering self-instability were sought.

CHAPTER 2

EXPERIMENT AND MEASUREMENT SYSTEMS

2.1 Swirl Injector Cold Test Facility

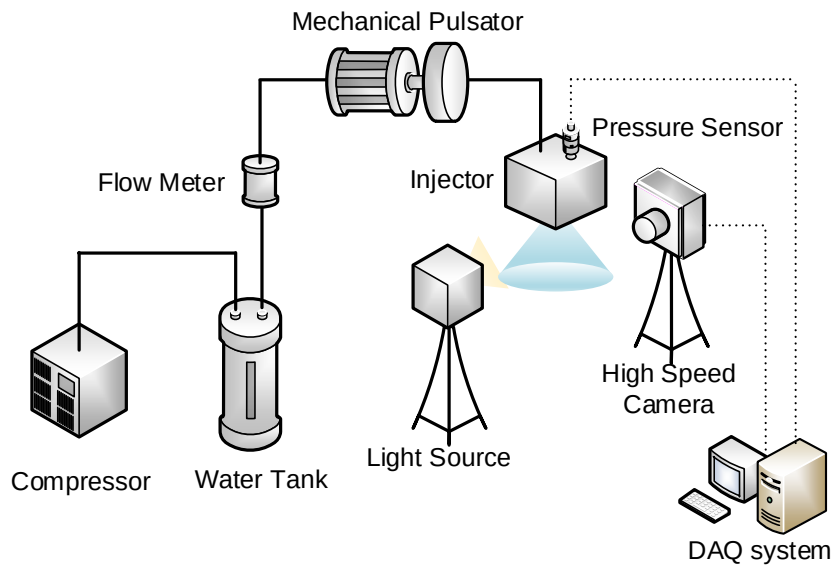

Fig. 2.1 Schematic diagram of the swirl injector cold test facility

Experimental apparatus of this study is as shown in Fig. 2.1. Water was used as test fluid. As shown in Fig. 2.1, water was sent to the injector by pressurized air using compressor. Water then entered the swirl chamber through the tangential inlet, rotated on the wall, and proceeded to the outside. The required flow rate was controlled by regulator (accuracy = ±0.02 atm) and measured by the flow meter

(Hoffer Flow Control, HO1/2X1/4A-.35-3.5-BP-1MX-MS-X, uncertainty = ± 0.49%) installed in the feed line. With static pressure sensor sensor (Valcom, VPRQ-A5-20Bar-4C, uncertainty = ± 0.8%) installed at the manifold of injector, differential pressure could be measured with conditions. To investigate flow self-oscillation phenomenon, backlight image technique was used to measure flow of the injector. For still shot images, lens (Canon EF 180mm F3.5L Macro USM) with camera (Canon EOS 7D) and stroboscope were used. For high-speed images, lens (Canon EF 180mm F3.5L Macro USM) with high-speed camera (Lavision, Highspeed Star8) and a continuous light source (Photron, HVC-SL) were used. At this time, the frame resolution was set at 5184 × 3456 pixels for still shot images and at 1024 × 1024 pixels for high-speed images. Also, high-speed images were taken at 6000 frames per second to measure the dynamic characteristics.

Droplet characteristic was also investigated to find the effect of self-oscillation in combustion related characteristics. To measure droplet characteristics, a microscope lens (Questar, VZ-QM1.VIS.BK7/MgF2 Corrector) with high-speed camera and continuous light source were used to obtain enlarged backlit images. Images were taken with 250 frame per seconds to prevent counting same droplets multiple times. The frame resolution of this images was set at 640 x 640 pixels, and imaging area was set at 3mm x 3mm. At this time, the detection point was set to 60 mm below and 81 mm right to the end of the orifice center. Because breakup of spray sheet was completed in 25 ~ 55 mm at all experimental cases, there was no problem in measuring droplet characteristics at 60mm below to the orifice. In addition,

because mass flow is concentrated in the direction of the sheet and the droplets are distributed in a hollow shape with typical single swirl injector, the measurement point where position is on the line of sheet direction could be representative of droplet characteristics of the swirl injector in this study. One of the obtained droplet image was shown in Fig. 2.2 (a). After detecting the area occupied by the droplet from the image, the diameter of the droplet was calculated with assuming droplet area as circle. At this time, the diameter was measured for some of the droplets in the image under several conditions to prevent errors. First, to measure the droplets in focus, droplets which had the intensity above threshold value was excluded. Next, the ellipse droplet of which ratio between the major axis and minor axis exceed 2 was excluded. When the ratio between the long axis and the short axis is large, it could be considered as just before secondary breakup. If the secondary breakup occurs, an error may occur because the number of droplets are doubled. Thus, this kinds of droplets were also excluded. Finally, the droplets cut by the sides of the image were excluded because the total droplet size could not be known. Droplets classified through these processes were marked with a red line as shown in Fig.2.2 (b). D10 (Mean droplet size) and SMD (Sauter Mean Diameter) were calculated from over 7000 droplets from 3000 images by Eq. (2.1) and Eq. (2.2) (Bayvel and Orzechowski, 1993).

$$D_{10} = \frac{\sum D_i n_i}{\sum n_i} \quad (2.1)$$

$$SMD = \frac{\sum D_i^3 n_i}{\sum D_i^2 n_i} \quad (2.2)$$

Where D_i is diameter of droplet i and n_i is the number of droplet with having diameter D_i, respectively.

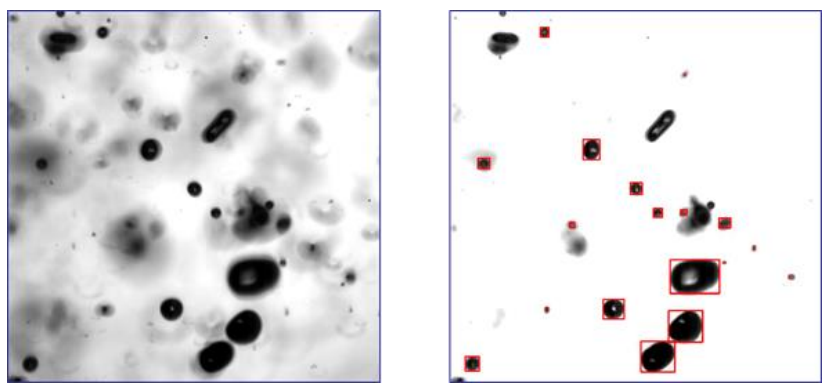

(a) (b)

Fig. 2.2 Original droplet image (a) and selected droplet image by MATLAB code (b)

2.2 Method for Dynamic Analysis of Internal Flow Image

For the dynamics analysis, internal and external flow images of the injector were used. At first, the internal flow image was investigated. As mentioned at Chapter 1, flow oscillating factors such as film hydrodynamics and swirl post acoustics, liquid-gas shear layer instability exist inside of a swirl injector. Therefore, to understand the cause of the instability more definitely, it was necessary to investigate the flow pulsation phenomenon inside the injector. Therefore, the image of the internal flow of the swirl chamber, as shown in Fig. 2.3, was taken using the backlight technique. From the figure, the light intensity exhibited a unique profile, showing a distinct boundary of intensity at particular locations. This profile was similar to Kenny's film thickness image. Kenny (2009) explained that the intensity derivative is either minimum or maximum at locations where the nozzle diameter edge distorted the background light. Using this information, the air core diameter, indicated by red arrows in Fig. 2.3, was obtained.

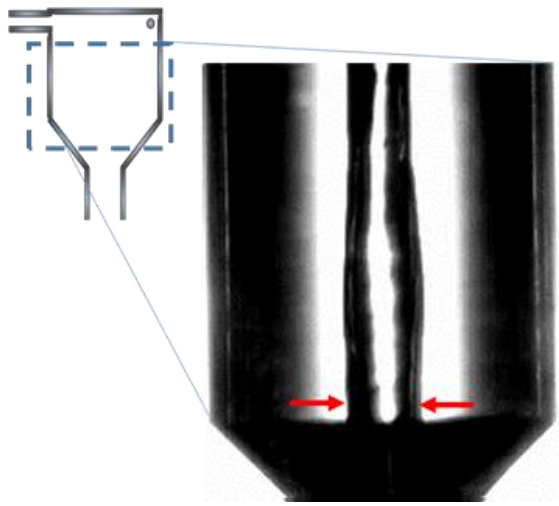

Fig. 2.3 Backlit image of internal flow at the swirl chamber

To find the dynamic characteristics, an analysis process shown in Fig. 2.4, was carried out. First, the points before the swirl chamber converging section, indicated by the red arrows in Fig. 2.4 (b), were chosen, and the air core diameter was calculated from the image. Next, images with 6000 frame per seconds were used to get the time domain air core diameter graph shown in Fig. 2.4 (c). From this graph, the self-oscillation amplitude of internal flow was obtained. To determine the dynamic characteristics, the Fast Fourier Transform (FFT) process was performed as shown in Fig. 2.4 (d). From this procedure, most predominant frequency at the internal flow was obtained and regarded as self-oscillation instability frequency.

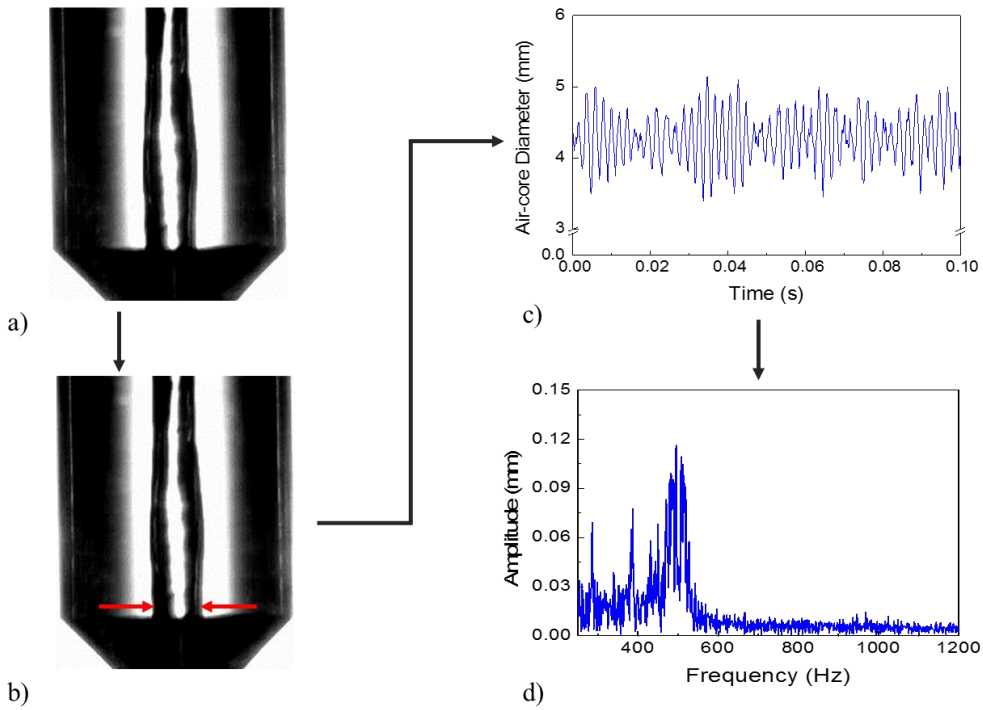

Fig. 2.4 Dynamic analysis process of internal flow: a) raw image, b) measuring point, c) air core diameter with time, d) FFT result.

2.3 Method for Dynamic Analysis of External Flow Image

The dynamic characteristics of the external flow also proceeded similarly to the internal flow case. The analysis process is shown in Fig. 2.4. Figure 2.4 (a) shows one of the raw images. The binarization of the original image was carried out to determine the surface of the external spray. Images with distinct surfaces were then taken, as shown in Fig. 2.4 (b). The spray angle was calculated from four points of the image: both ends of the injector tip and both ends of surface points which were 6 mm below the injector tip. When the same process was applied to the entire image, the time domain spray angle graph, shown in Fig. 2.4 (c), was obtained. Through this graph, the amplitude of self-oscillation instability at the external flow was obtained. FFT was also performed as shown in Fig. 2.4 (d). It was found that the peak frequency existed at external spray, similar to self-oscillation at the internal flow case. The frequency at this time was defined as the self-oscillation instability frequency of the external flow and analysis was performed.

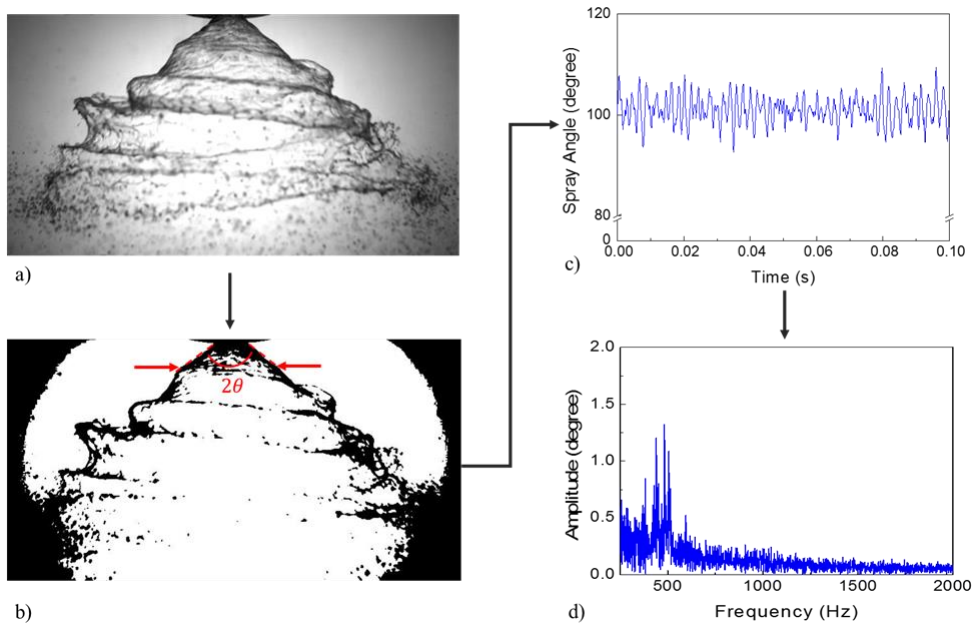

Fig. 2.5 Dynamic analysis process of external spray: a) raw image, b) binarization, c) spray angle with time, d) FFT result

2.4 Hydraulic Mechanical Pulsator

To find the dynamic characteristics of an injector, a device which can make external pulsation with specific frequency continuously was needed. This kind of device called pulsator. Generally, the pulsator is classified according to the drive type and there are four main types of pulsator: hydro-dynamic, acoustic, inertial and self-oscillating pulsator (Bazarov et al., 2007). Table 1 shows the advantages and disadvantages of pulsator with drive type.

Table 2.1 Drive advantages and disadvantages (Bazarov et al., 2007)

Type of Drive	Advantages	Disadvantages
Hydro-dynamic	- Low power requirements - High amplitude is possible - High frequency is possible - Strong pulsation in compressible fluids - Smooth and continuous frequency control - Low noise during operation	- Non-Harmonic pulsation - Wasted model liquid - Possible leakages - High friction parts - High speed rotation - Cannot be used with cryogenic, toxic, and hypergolic liquids

Acoustic	- Harmonic pulsations - Can be used with any liquid	- Weak pulsation amplitude - Frequency fixed by actuator - High-power drive - High noise - Primarily for small scale experiments
Inertial	- No leaks - No friction - Wide frequency range - Can be used with any liquid	- Requires high power drive - Generates high level of noise
Self-oscillating	- Absence of external drive - Can be used with any liquid - Can be used with gases	- Dependence of frequency, amplitude and even the presence of pulsation on operational parameters of the studied flow

In this study, hydraulic mechanical pulsator as shown in Fig. 2.6 was installed at the feedline because of advantages with strong pulsation. Rotating disk connected to the motor rotated. When the hole at the disk coincided with the port hole, a part of the fluid escaped to the outside. When the hole at the disk did not coincide with the port hole, all of the fluid directly moved to the injector. This procedure could make a regular pressure pulsation. By changing the rpm of the motor, pulsation

frequencies could be controlled. Pressure fluctuation amplitude of pulsator with respect to excitation frequency is same as Fig. 2.7. Fluctuation amplitude was almost same, with 20 percent of static pressure below 800 Hz excitation frequency. Therefore, dynamic characteristic of excitation frequency range of 100 Hz to 800 Hz was investigated in this study.

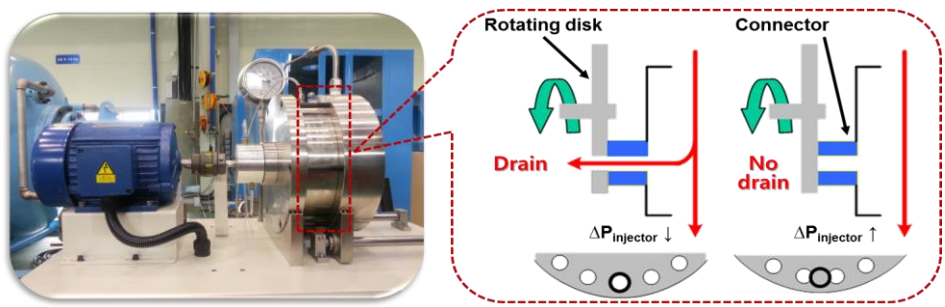

Fig. 2.6 Principle of hydraulic mechanical pulsator

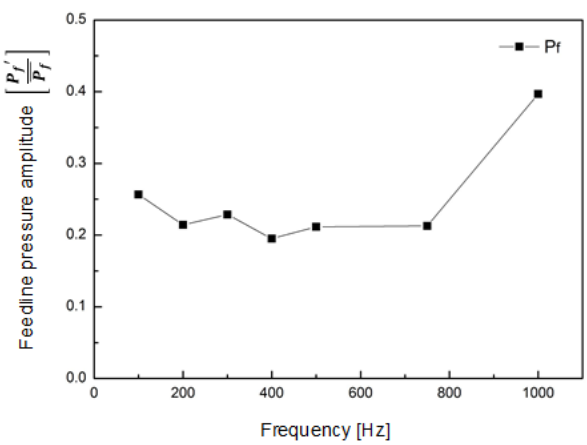

Fig. 2.7 Pressure fluctuation amplitude of pulsator with respect to excitation frequency

CHAPTER 3

CHARACTERISTICS OF SELF-OSCILLATION IN THE SWIRL INJECTOR FLOW

3.1 Objectives and Test Conditions

There have been many developments in the space launch vehicle industry, and there has been increasing interest in manned launch vehicle projects such as space tourism and space station business. As a result, the stability of a rocket launch vehicle has become more important. One of the most dangerous instabilities of a launch vehicle is the combustion instability of the engine. To solve the combustion instability, baffle or acoustic cavities are generally used. However, these methods decrease the payload mass of the launch vehicle owing to the additional mass on engine structure. The method of changing the dynamic characteristics of an injector of a launch vehicle has the advantage that it does not have a great influence on the engine efficiency because no additional mass is added.

Generally, the atomization instability of an injector is closely related to combustion instability. Anderson et al. (1998) confirmed that the atomization frequency in an impinging jet injector is related to the frequency of combustion instability. Ahn et al. (2012) experimentally confirmed the importance of injector dynamics. By comparing the frequency of combustion instability to the instability

frequency calculated from the injector dynamics, they suggested that the characteristics of injector dynamics might be related to the actual combustion instability. In addition, a few groups performed experimental studies by using an external pulsating device to find more detailed characteristics of the injector transfer function in real situations (Wilson et al., 2009, Fu et al., 2010, Khil et al., 2012, Chung et al., 2016, Yang et al, 2018).

However, the experimental results on self-instability of swirl injector flow, especially internal flow, are still insufficient. Therefore, the internal flows of a swirl injector with self-unstable condition were experimentally investigated in this chapter. Through experiments of unstable characteristics with changing pressure and injector structure, data of unstable flows with tangential velocity were acquired and the parameters affecting dynamic characteristics of this type of sheet flow were examined.

Experiments were performed with various conditions to find out main parameters which are related on self-oscillation of swirl injector. Basic geometry of the swirl injector was as follows: the swirl chamber length L_s was 19 mm, swirl chamber diameter D_s was 18 mm, orifice diameter D_o was 6 mm, the number of tangential inlet ports N_t was 3, and tangential inlet port diameter D_t was 1 mm. With this base geometry, various structures as shown in Table 3.1 was used. In addition, pressure difference between the injector and ambient air was varied from 1 atm to 7 atm to find the effect of the flow rate. The ambient pressure was fixed at 1 atm. As the images of internal flows had to be taken, injectors were made of a transparent

acrylic material. Under these conditions, images of internal flow were taken by using a backlight image technique using high-speed camera at 6000 frames per second. At this time, the frame resolution was set at 512 x 512 pixels for internal image.

Table 3.1 Geometries of swirl injector in Chapter 3

Parameter	Dimension
Number of tangential inlet ports, N_t	2, 3, 4, 5
Inlet port diameter, D_t [mm]	1, 2, 3
Swirl chamber length, L_s [mm]	19, 24, 28
Swirl chamber diameter, D_s [mm]	18, 21
Orifice length, L_o [mm]	10
Orifice diameter, D_o [mm]	6, 9
Converging angle, α_c [°]	45

3.2 Relation between Internal and External Flow Characteristics

Based on method explained at Chapter 2.2, self-oscillation instability characteristics of the internal flow was measured with respect to mass flow rate under the conditions of swirl chamber diameter of 19 mm and swirl chamber length of 28 mm. Black square symbols of Fig. 3.1 (a) shows the self-oscillation amplitude with respect to mass flow rate obtained from the time domain air core diameter graph. During this time, the amplitude was calculated from the normalized root mean square (RMS) deviation value, as expressed in Eq. (3.1).

$$Amp_{\text{internal}} = \frac{\sqrt{\sum_{i=1}^{n}\left(D_{a,i} - D_{\ a,mean}\right)^2}}{D_{\ a,mean}}, \tag{3.1}$$

where $D_{a,i}$ is air core diameter of each image i and $D_{a,mean}$ is averaged air core diameter.

For sinusoidal waves, peak-to-peak amplitude is proportional to the RMS value. Hence, the fluctuation amplitude could be compared using the above equation. Consequently, the phenomenon that the fluctuating amplitude decreased slightly with mass flow rate increase for internal flow cases was confirmed. The phenomenon that the fluctuation frequency increased proportionally with increase of flow rate for internal flow cases, as shown in black square symbols of Fig. 3.1 (b) was also found.

Self-oscillation instability characteristics of the external spray were also

measured by changing the mass flow rate under the conditions of swirl chamber diameter of 19 mm and swirl chamber length of 28 mm. Red circle symbols of Fig. 3.1 (a) shows the amplitude with mass flow rate obtained from the time domain spray angle graph for external spray. During this time, the amplitude was calculated from the normalized root mean square (RMS) deviation value, as expressed in Eq. (4.1).

$$Amp_{\text{external}} = \frac{\sqrt{\sum_{i=1}^{n}(2\theta_i - 2\theta\ mean)^2}}{2\theta_{mean}}, \tag{4.1}$$

where θ_i is spray angle of each image i and θ_{mean} is averaged spray angle.

Consequently, it was confirmed that the fluctuating amplitude decreased slightly with increasing mass flow rate for external and internal flow cases. It was also confirmed that the self-oscillation frequency increased proportionally with increasing flow rate for external and internal flow cases, as shown in red circle symbols of Fig. 4.1 (b). It can be observed from this graph that the unstable characteristic of the external spray is similar to that of internal flow. Consequently, it can be seen that the instability characteristics of the external spray and the internal flow are due to the same causes. Next section, experiments with various injector geometries were carried out for more detailed analysis about the self-oscillation instability of the injector.

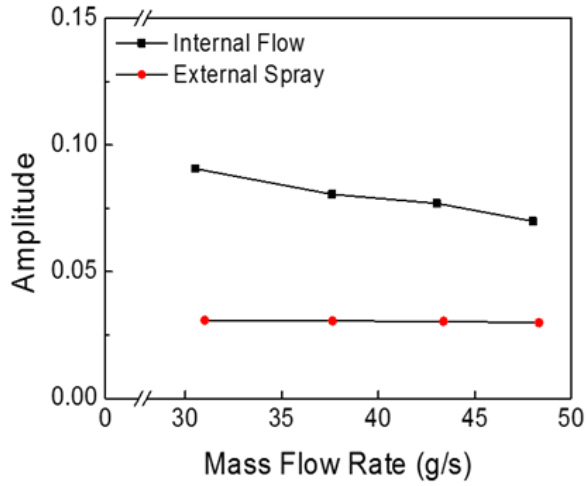

(a)

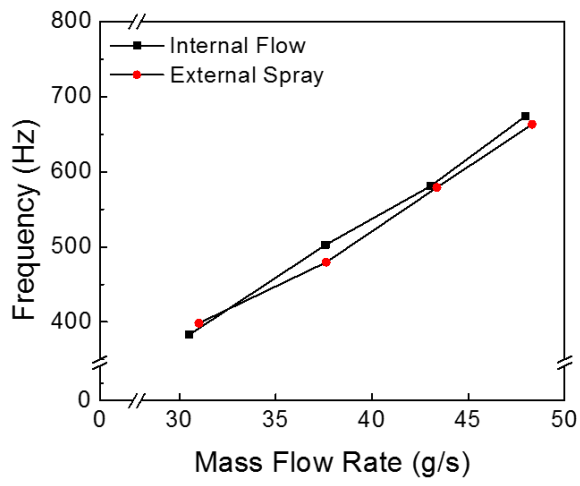

(b)

Fig. 3.1 External spray angle and internal air core diameter (a) fluctuation amplitude and (b) frequency with mass flow rate at *Ls* = 28 mm case

3.3 Main Parameters Affecting Self-oscillation

The effect of swirl chamber geometry on self-oscillation was investigated at first. Figure 3.2 shows the injector self-oscillation instability characteristics with mass flow rate changing the swirl chamber length to 19 mm, 24 mm, and 28 mm. As shown in Fig. 3.2 (b), the swirl chamber length had no effect on mean fluctuation frequencies; however, swirl chamber length significantly affects the fluctuating amplitude. From the Fig. 3.2 (a), as the swirl chamber length increased, the fluctuating amplitude became larger.

Figure 3.3 shows the injector self-oscillation instability characteristics with respect to mass flow rate changing the swirl chamber diameter to 18 mm and 21 mm. It can be seen that the swirl chamber diameter also had no effect on self-oscillation frequencies as shown in Fig. 3.3 (b). However, as shown in Fig. 3.3 (a), swirl chamber diameter affected the fluctuating amplitude to some extent. As the swirl chamber diameter increased, the fluctuating amplitude became smaller. Consequently, it was found that as the swirl chamber length to diameter ratio increased, the flow became more unstable. This phenomenon was also presented in Kim (2008) 's previous study. They confirmed that the flow instability occurs owing to the axial friction at the injector wall, which increases as the swirl chamber length to diameter ratio increases.

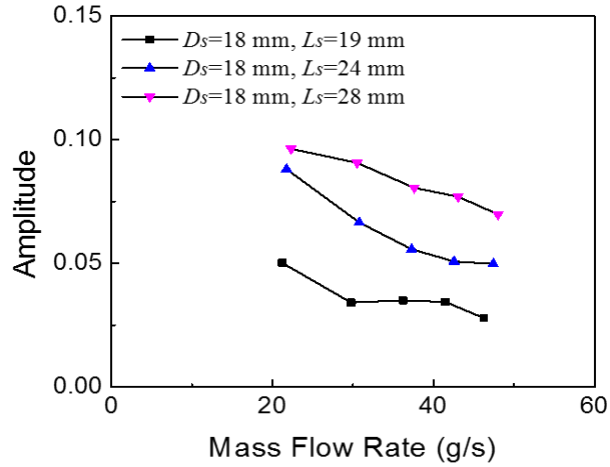

(a)

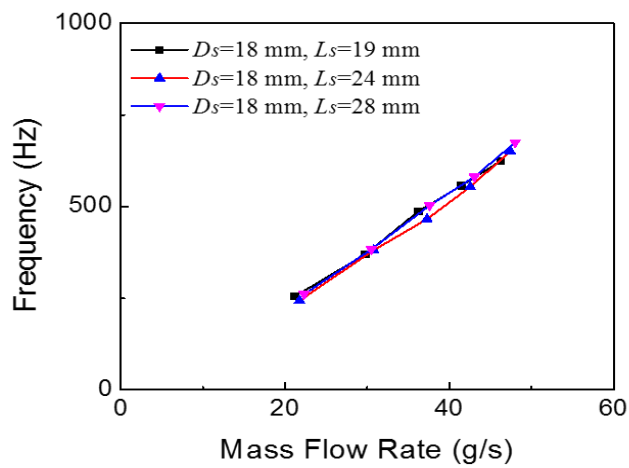

(b)

Fig. 3.2 (a) Injector self-oscillation amplitude and (b) frequency with respect to mass flow rate varying swirl chamber length to 19 mm, 24 mm, and 28 mm

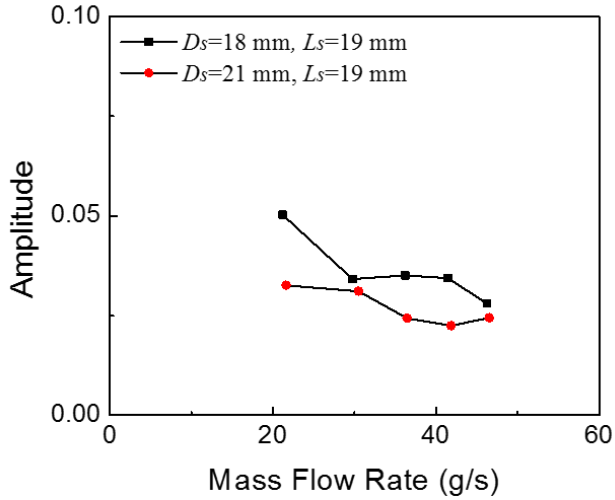

(a)

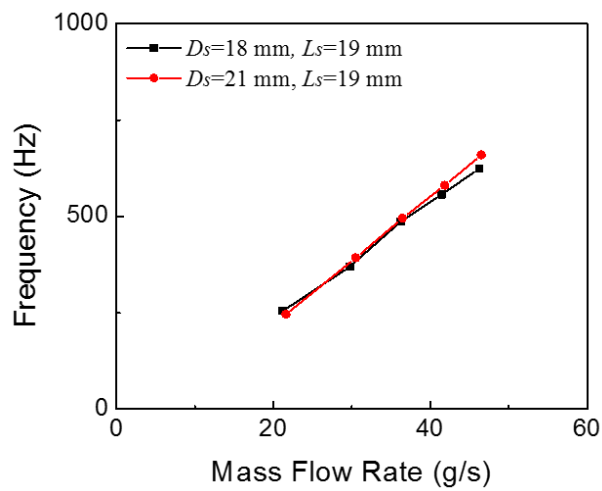

(b)

Fig. 3.3 (a) Injector self-oscillation amplitude and (b) frequency with respect to mass flow rate varying swirl chamber diameter to 18 mm, and 21 mm

The influence of the inlet geometries on instability was then examined. Figure 3.4 shows the results with changing the tangential inlet port diameter to 1 mm, 2 mm, and 3 mm. Figure. 3.4 (a) shows that the fluctuating amplitude decreases slightly as the mass flow rate increases and inlet port diameter decreases. Figure 3.4 (b) shows that the fluctuation frequency varies unlike the swirl chamber case. The frequency decreases as the inlet port diameter increases. Figure 3.5 shows the results with mass flow rate changing the numbers of tangential inlet ports to 2, 3, 4, and 5. As shown in Fig. 3.5 (a), there is no clear relation between the numbers of inlet ports and fluctuating amplitude; however, the fluctuation frequency decreases as the numbers of inlet ports increases as shown in Fig. 3.5 (b). Consequently, the phenomenon that the mean fluctuation frequency was inversely proportional to the swirl injector inlet area A_{in} was found.

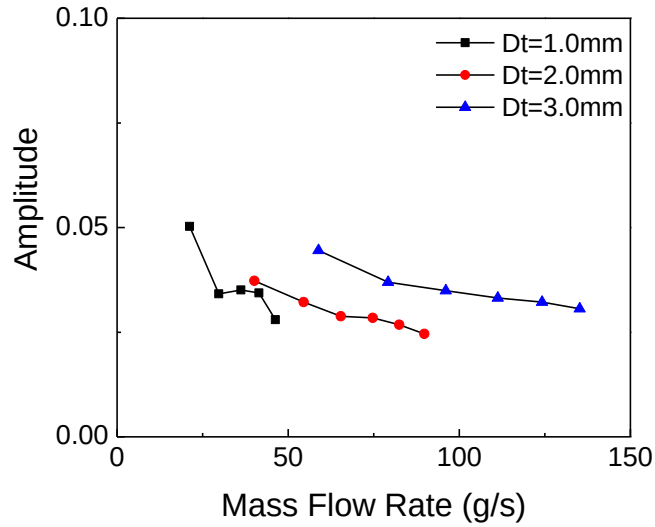

(a)

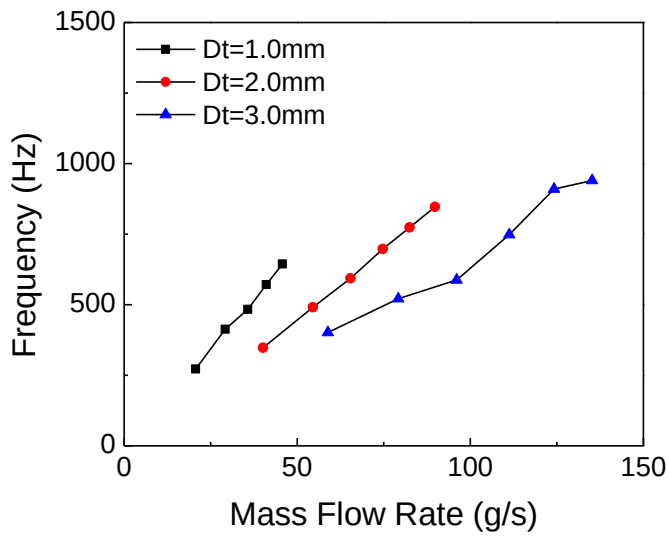

(b)

Fig. 3.4 (a) Injector self-oscillation amplitude and (b) frequency with respect to mass flow rate varying tangential inlet port diameter to 1 mm, 2 mm, and 3 mm

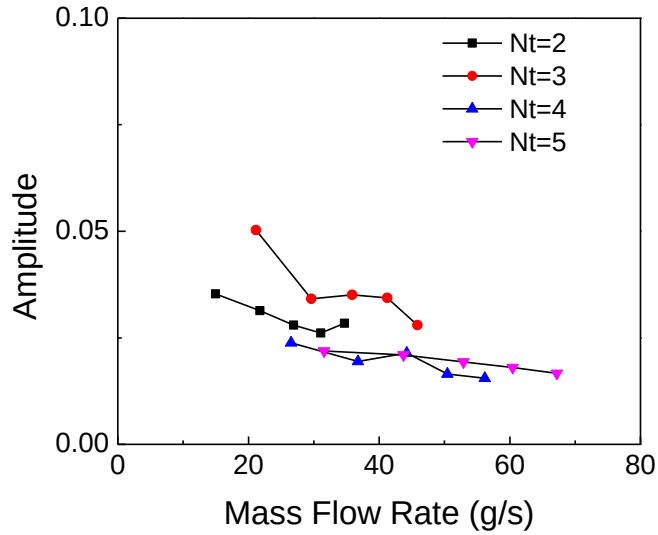

(a)

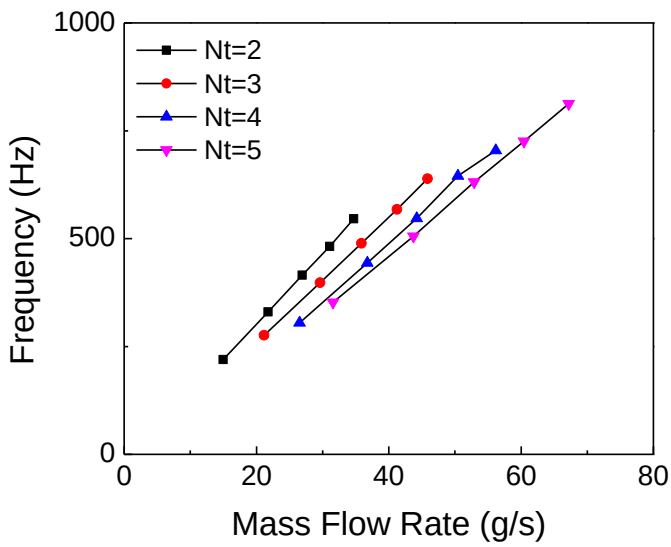

(b)

Fig. 3.5 (a) Injector self-oscillation instability amplitude and (b) frequency with respect to mass flow rate varying the number of tangential inlet port to 2, 3, 4, and 5

The influence of the outlet geometry was also examined. Figure 3.6 shows the results with mass flow rate changing the orifice diameter to 6 mm and 9 mm. The fluctuating amplitude does not change significantly, similar to the number of tangential inlet port case. However, the fluctuation frequency decreases as the orifice diameter increases, which means increase of the injector outlet area A_{out}.

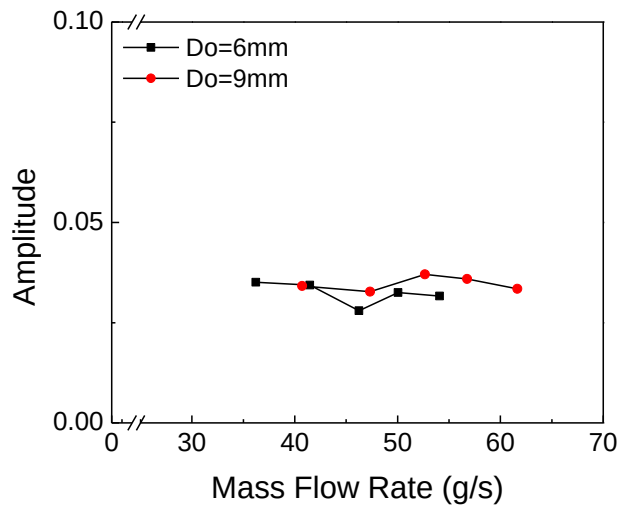

(a)

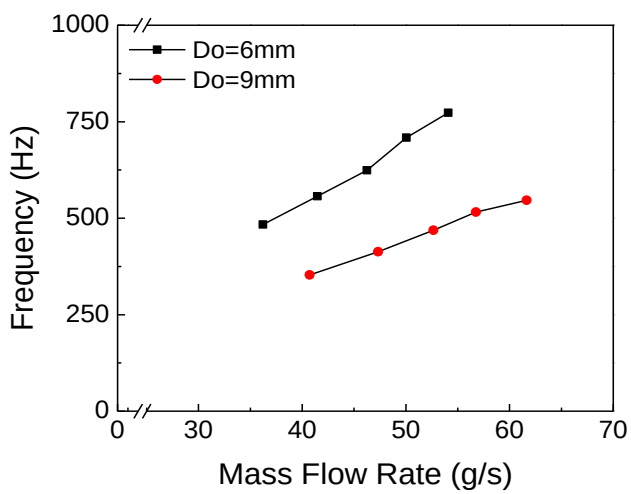

(b)

Fig. 3.6 (a) Injector self-oscillation instability amplitude and (b) frequency with respect to mass flow rate varying orifice diameter to 6 mm and 9 mm

In summary, components such as mass flow rate, swirl chamber length and diameter, and tangential inlet port diameter were found to have effect on the fluctuating amplitude. These components had one thing in common that they all were related to the momentum of the swirl injector. As the mass flow increases and the tangential inlet port diameter decreases, the inlet velocity increases. As the swirl chamber diameter increases, the angular momentum increases. As the swirl chamber length increases, the angular momentum at the orifice exit reduces more because of friction from liquid-gas shear layer. The tangential velocity of the sheet flow increases with increasing angular momentum, that is, high tangential velocity affects stable flow. Based on this, the entire experimental results were expressed as non-dimensionalized parameters as shown in follow Eq. (3.2).

$$\mathrm{AMP} = 34.87 \left(\frac{L_s}{D_s}\right)^{2.54} \left(\frac{D_s}{D_o}\right)^{-0.93} {Re_{in}}^{-0.57} \tag{3.2}$$

As shown in Fig. 3.7, it was confirmed that the experimental value and the value calculated from Eq. (3.2) are quite consistent. Each dimensionless parameter in Eq. (3.2) were dealt in more detail. First, the length-to-diameter ratio of the swirl

chamber was a parameter related to the friction at the gas-liquid boundaries. With this ratio increased, the instability amplitude was increased because the area of the gas-liquid interface was increased. Next, the swirl chamber to orifice diameter ratio was a parameter related to the angular momentum. As it increases, the momentum in the swirl chamber increases. As a result, the self-oscillation amplitude decreases as the angular momentum. Lastly, Reynolds number at the inlet was a parameter related to the initial liquid momentum. As the angular momentum in the swirl chamber increases, the unstable amplitude decreases. As a result, it was found that the amplitude of self-oscillation decreases as the momentum of the liquid increases, making the flow more robust to external disturbances.

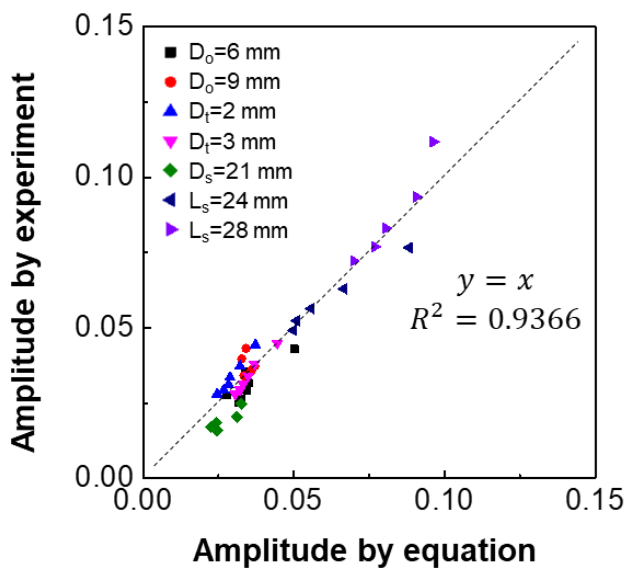

Fig. 3.7 Relation of injector self-oscillation instability amplitude obtained from experiment and empirical equation

In addition, three more components, mass flow rate, inlet area A_{in}, and outlet area A_o, were found to have effect on the mean fluctuation frequency. These three components had one thing in common that they were related to the axial velocity of swirl injector. The axial velocity of swirl injector can be expressed as shown in Eq. (3.3).

$$U_{ax} = \frac{\dot{m}}{\rho(A_o - A_a)} \tag{3.3}$$

From Eq. (3.3), it can be easily found that the axial velocity is proportional to the mass flow rate, and inversely proportional to the orifice area. The relationship between the inlet area and the axial velocity can be explained using several relations.

$$K = \frac{\pi R d_o}{2 N_t A_t} \tag{3.4}$$

$$\epsilon = \frac{A_e}{A_o} = \frac{A_o - A_a}{A_o} = 1 - \frac{A_a}{A_o} \tag{3.5}$$

$$K = \frac{(1-\epsilon)\sqrt{2}}{\epsilon\sqrt{\epsilon}} \tag{3.6}$$

When inlet area increases, the injector geometric constant K, defined in Eq. (3.4), decreases. Using the maximum flow principle in swirl injector, the relation between the injector geometric constant and orifice filling coefficient ε is expressed in Eq. (3.6) (Bayvel, 1993). To sum up, the orifice filling coefficient increases as the

inlet area increases, and by referring to the definition of the orifice filling coefficient, expressed in Eq. (3.5), as the air core sectional area increases, the axial velocity decreases. This means that axial velocity is inversely proportional to the inlet area. Supposing that the injector self-oscillation frequency is proportional to the axial velocity, the trends observed in the experimental results can be explained. To obtain a precise verification, axial velocities were obtained by substituting the air core diameter, determined from the experimental image, into Eq. (3.3). The mean fluctuation frequencies with axial velocities for all experimental cases are shown in Fig. 3.8. During this time, the axial velocity was divided by the hydraulic diameter D_H (= $D_o - D_a$) at orifice to make its unit same as frequency. Consequently, it was found that the mean fluctuation frequency was proportional to the axial velocity of the swirl injector. In addition, the slope, which was expressed in the same way as Strouhal number in Eq. (3.7), remained constant at a value of approximately 0.235 for these study cases.

$$Slope = \frac{fD_H}{U_{ax}}, \tag{3.7}$$

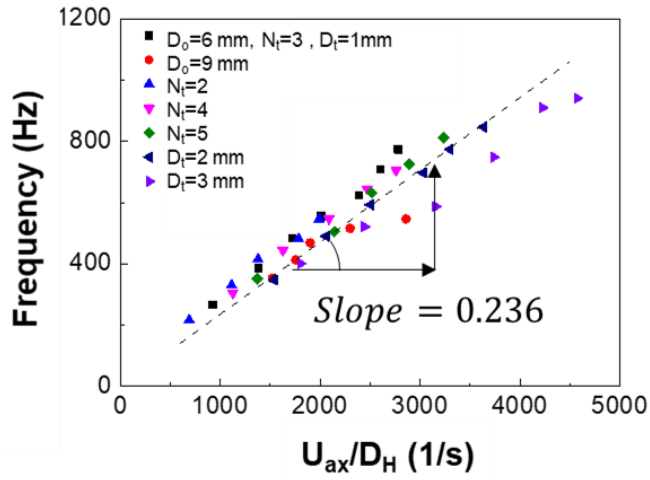

Fig. 3.8 Injector self-oscillation frequencies with respect to axial velocities divided by hydraulic diameters at orifice for all experimental cases

3.4 Discussion on Self-oscillation Phenomenon

There are various causes of swirl injector self-oscillation instability, such as surface wave resonance and unstable sheet by the aerodynamic or hydrodynamic force generated in the injector. In the case of self-oscillation instability in this study, even if the length and diameter of the swirl chamber changed, there were no changes in unstable frequency as shown in Figs. 3.2 and 3.3. This result indicates that the self-oscillation instability is caused by the external sheet instability rather than the internal wave resonance effect in the swirl chamber. The experimental results show that the flow characteristics were similar to the preferred mode of thin liquid sheet owing to aerodynamic force. According to Dombrowski et al. (1963), the thin liquid sheet flow develops as wavy flow caused by the influence of the pressure force, surface tension force, inertial force, and shearing force. The increase in main frequency owing to the increase in flow velocity observed in this study is caused by an increase in the wave velocity as the external flow velocity increases. This result is confirmed by Lienemann et al. (2007)'s attenuating liquid sheet test.

In the case of the external flow of the swirl injector in this study, there existed a tangential velocity term unlike the general fan-sheet flow. The tangential velocity did not affect the axial wave frequency of the sheet, but it affected the total liquid momentum. As the tangential velocity increased, the flow became robust to external disturbance. In the study of Im et al. (2009), although a gas-liquid swirl coaxial injector was used, it was confirmed that as the liquid momentum increases in the

sheet type spray, the resistance to disturbance due to air flow increases. In addition, self-oscillation instability decreases as the liquid momentum increases in sheet type spray.

In summary, it was found that the characteristics of self-oscillation instability in the swirl injector appeared on a principle similar to the waves at sea level. At sea level, waves are generated due to the speed difference caused by wind as shown in Fig. 3.9 (a), and in the flow inside the injector, friction is generated at the interface due to the speed difference caused by the axial speed that the liquid flows outward, resulting in wave-shaped unstable flow as shown in Fig. 3.9 (b). At sea level, it is known that gravity acts as a restoring force, and a smooth wave shape close to a sine wave could be generated. In the case of the flow inside the swirl injector, centrifugal force due to swirl momentum acted as a restoring force, so that a smooth wave was formed. In addition, since the centrifugal force acted as a restoring force, it was appeared that the instability amplitude decreased as the swirl moment of the liquid increased in the experiment.

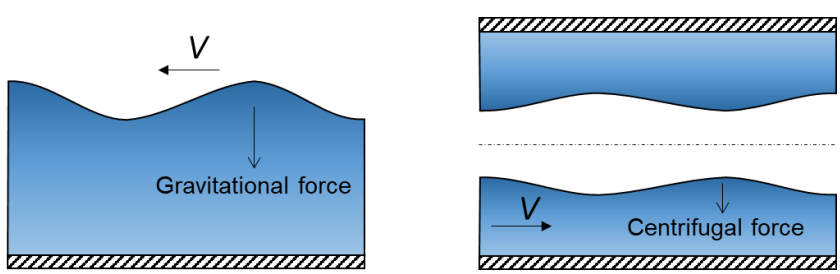

Fig. 3.9 Comparison of wavy flow (a) at the sea level and (b) at the swirl injector

CHAPTER 4

EFFECT OF SELF-OSCILLATION ON THE SWIRL INJECTOR FLOW CHARACTERISTICS

4.1 Objectives and Test Conditions

As mentioned in Chapter 3, because of a thin sheet flow, the spray could be easily affected by external factors, such as aerodynamic force, and became unstable. This instability can make the injector characteristics different from the designed values. If an injector with serious instability is used for combustion, it can cause serious engine failure. Therefore, research on instabilities in injector flow is important.

Studies about thin liquid sheet have investigated wave type instability. However, these sheet-flow studies focused mainly on the prediction of the initial formation of wave instability and breakup. There were some limitations to investigating dynamic characteristics, which are associated with combustion instability. Because combustion instability is a phenomenon that occurs when the flow and combustion characteristics are acoustically coupled, determining the instability frequency and its effects on the spray is important. The branch of study related to this problem is called injector dynamics as mentioned in Chapter 1. However, studies about the effects of self-oscillation wave instability on the dynamic characteristics of an injector have

been lacking because injector dynamics studies have been focused mainly on instability from the internal structure of the swirl injector. Therefore, in this chapter, the effects of self-oscillation instability on the actual atomization process and on the dynamic characteristics of swirl injector were examined experimentally.

The geometry of the swirl injector in this chapter was as follows: the swirl chamber length L_s was 19 mm, the swirl chamber diameter D_s was 18 mm, the orifice diameter D_o was 9 mm, the number N_t of tangential inlet ports was 3, and the tangential inlet port diameter D_t was 1 mm. The condition of the experiment was as follows: the injector pressure drop P_m was 3 atm, the mass flow rate $\dot{m}$ was 40.5 g/s, and the ambient pressure was fixed at 1 atm.

4.2 Spray Characteristics with Self-oscillation Instability

4.2.1. Effect of Self-oscillation on Liquid Sheet Flow

The external sheet of a swirl injector was confirmed to be wavy due to self-oscillation instability, and the instability frequency of the swirl injector was confirmed to be proportional to the axial velocity at the orifice exit from previous Chapter 3. For this experiment, the self-oscillation frequency for the experimental condition was set at 312 Hz. To understand the effect of this instability on the spray flow, wave propagation at the external sheet flow was investigated. Measurement of wave characteristics was done via the following process. First, the average sheet position shown by the yellow line in Fig. 4.1 (a) was obtained from the average spray angle. The edge point of the sheet at the measuring position was then obtained from a backlit image. Because of the drastic change in intensity at the boundary of the liquid sheet, the edge point could be easily determined. Finally, the distance between the edge point and average sheet position of each image was measured as the wave amplitude. To determine the effect of instability with respect to sheet progression, wave amplitudes at five points on the sheet surface, positioned from 1.8 mm to 15.2 mm below the orifice tip, as shown in Fig. 4.1 (b), were measured with respect to time using a high-speed camera.

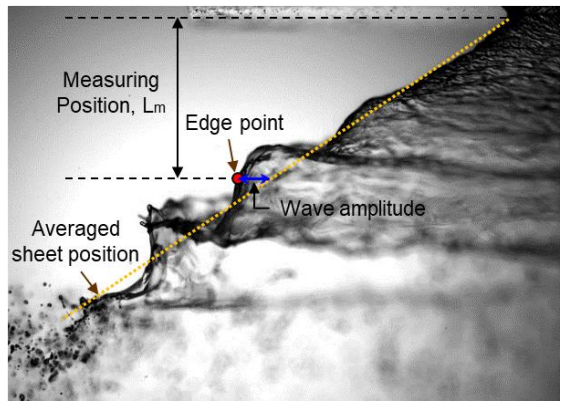

(a)

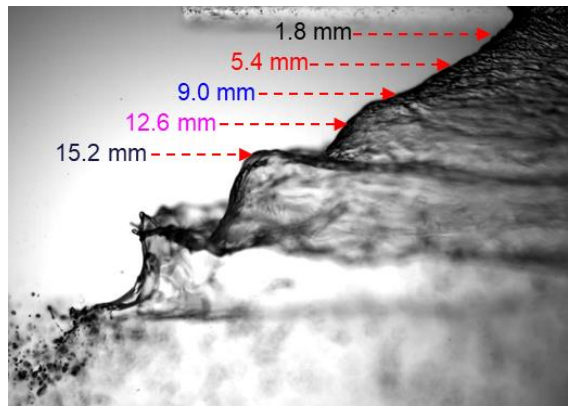

(b)

Fig. 4.1 (a) Wavy sheet spray image and (b) detection points

The result of this wave fluctuation with respect to position is shown in Fig. 4.2. The fluctuation amplitude can be observed to have increased with sheet progression, because of the characteristic of the thin liquid sheet. For thin liquid film flow, the displacement y of a plane sheet at a distance x is known to be able to be expressed as Eq. (4.2) (Dombrowski, and Johns, 1963).

$$y = T \ \sin(\mathrm{k}x + \theta_p),$$

$$y = T_0 \exp(f) \sin(\mathrm{k}x + \theta_p), \tag{4.2}$$

where T, T_0, f, n, and ε are the wave fluctuation amplitude, initial wave fluctuation amplitude, total growth of wave, wave number, and phase angle, respectively.

According to linear theory, four forces exist on the sheet: pressure, surface tension, internal, and viscous force, and because of the interaction of these aerodynamics forces, wavy flow forms and wave amplitude grow with sheet progression until the sheet breaks up (Dombrowski, and Johns, 1963).

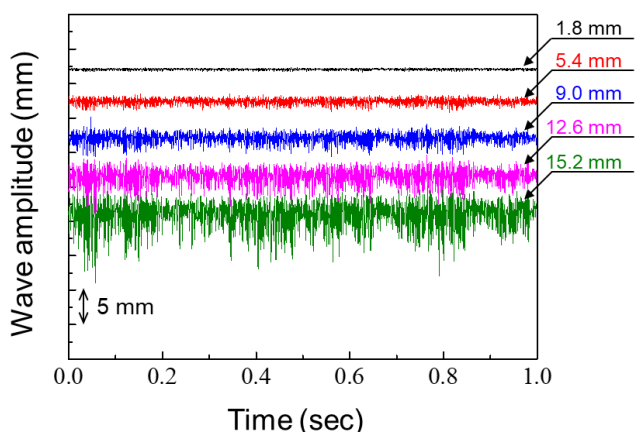

Fig. 4.2 Wave amplitude with respect to time for various axial positions

To see these characteristics in more detail, fast Fourier transform (FFT) was conducted. From Fig. 4.3, the self-oscillation frequency, 312 Hz, was confirmed to have remained despite the movement of the flow. Only the peak amplitude at the self-instability frequency had gradually increased as the flow was moving. From this result, self-oscillation frequency was determined to affect external sheet flow.

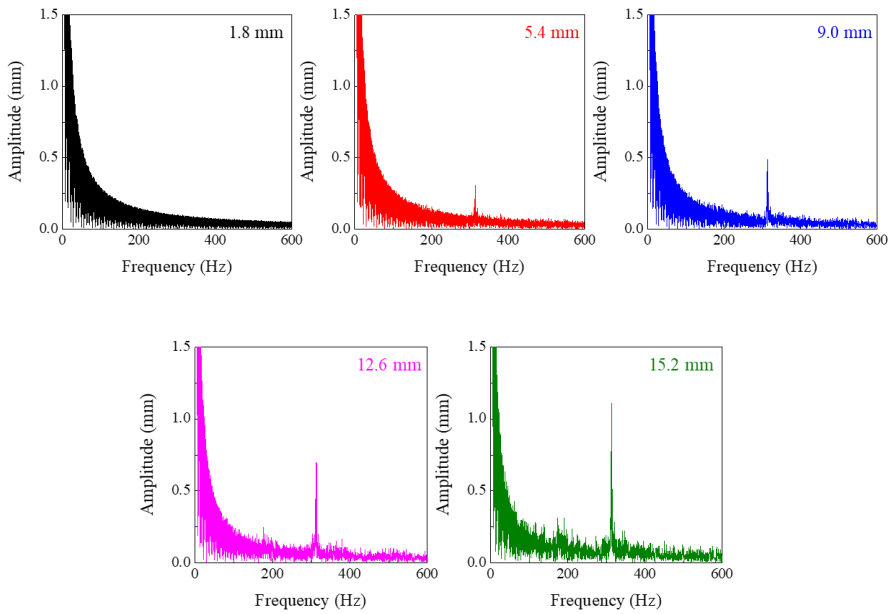

Fig. 4.3 FFT result of wave amplitude fluctuation for various axial positions

4.2.2. Effect of Self-oscillation on Breakup Length

The effect of self-oscillation on liquid sheet breakup was then investigated. Because the breakup length of an injector is a factor that relates to the combustion area, it is important for determining the size of the combustion chamber. If the breakup length is shorter or longer than the designed value, problems such as reduced engine efficiency or damage on the chamber wall could occur. Breakup of swirl injector spray is known to occur at each half-wavelength position (Fraser et al., 1962). In this study, the sheet also detached at the half-wave position and was broken into ligament and droplets, as shown in Fig. 4.4.

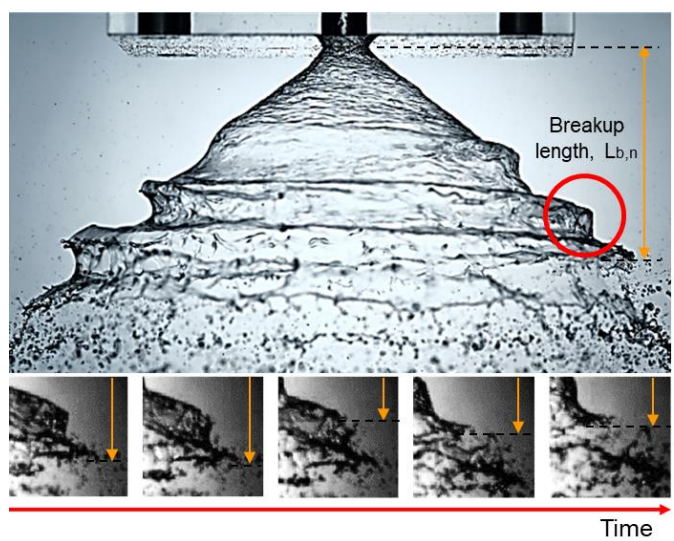

Figure 4.4 Spray detachment at half-wave position

The axial distance between the injector tip and the end of the spray sheet was defined as the breakup length, as shown in Fig. 4.4. The breakup length with respect to time was obtained from high-speed images taken at 6000 frames per second, as shown in Fig. 4.5.

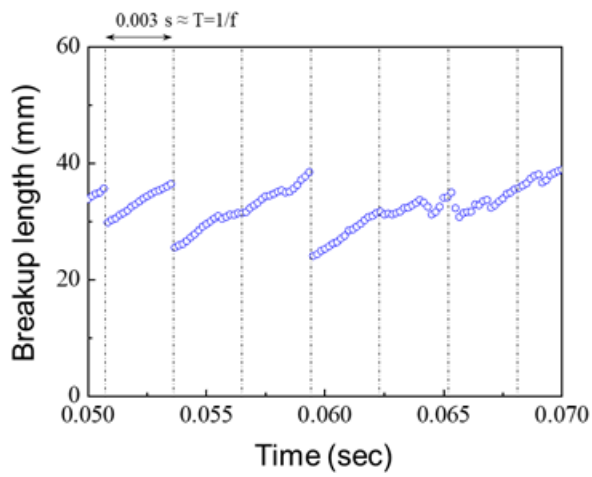

Figure 4.5 Breakup length with respect to time

A periodical phenomenon of gradual increase and rapid decrease in breakup length was observed throughout the measurement time. As shown in Fig. 4.6, the breakup was determined to have occurred at 0.003 s intervals, which is the same as the inverse of the self-oscillation frequency, 312 Hz. This trend seems to be because the wave period was the same as the self-instability frequency of the injector, and thus breakup occurred at the half-wave position repeatedly. Through this observation, the self-oscillation frequency was confirmed to have an influence on the breakup

length. However, at the time between 53 to 59 ms, as shown in Fig. 4.5, the breakup occurred two times later than the ordinary period. To discover the reason, breakup images at 59 ms were examined, and an unusual phenomenon was observed. Figure 4.6 shows that two waves could be detached at a single time. Although breakup does not always occur at the same location, the effect of self-oscillation on breakup length can be said to clearly remain as a periodical characteristic.

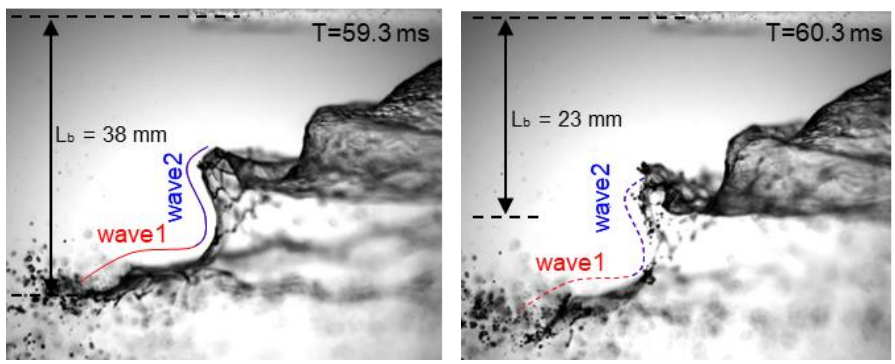

(a) (b)

Fig. 4.6 Breakup images at (a) 59.3 ms and (b) 60.3 ms

4.2.3. Effect of Self-oscillation on Ligament and Droplet Formation

The effect of self-oscillation on ligament and droplet formation was then investigated. Normally, ligaments are known to be detached from the liquid sheet and disintegrate into droplets when sheet disintegration occurs because of wave phenomena (Bayvel and Orzechowski, 1993). This sheet disintegration process consists of three parts: sheet progression, ligament detachment, and conversion to droplets. This process also occurred in this study, as shown in Fig. 4.7. Remarkably, the time of ligament-to-droplets conversion was relatively very short. After breakup, sheet progression continued for about 2 ms, and detachment of ligament occurred. At that time, the ligament was converted into droplets rapidly, within 0.5 ms. The remaining sheet then progressed for 2 ms. This whole process was repeated throughout the measurement time.

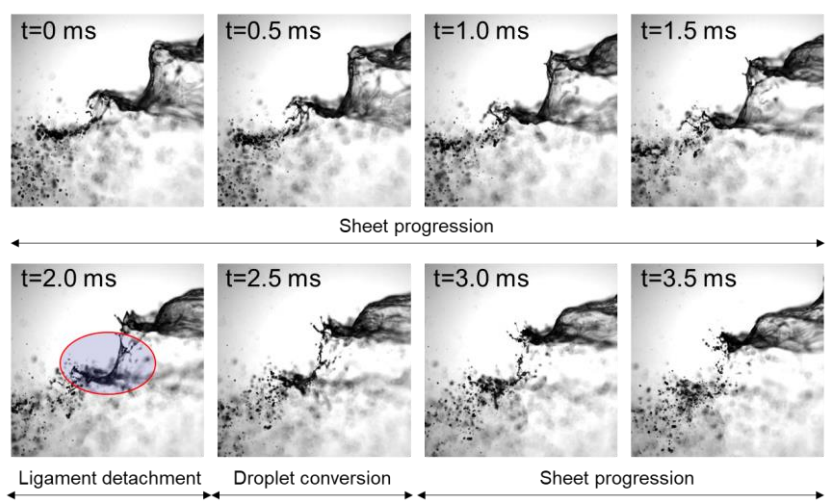

Fig. 4.7 Breakup process at the end of spray sheet

Next, spray front images were investigated to found ligament breakup process. As a result, it was observed that the separation of ligament occurred first at the weak point as shown in red circle area of Fig. 4.8. The ligament was then completely separated.

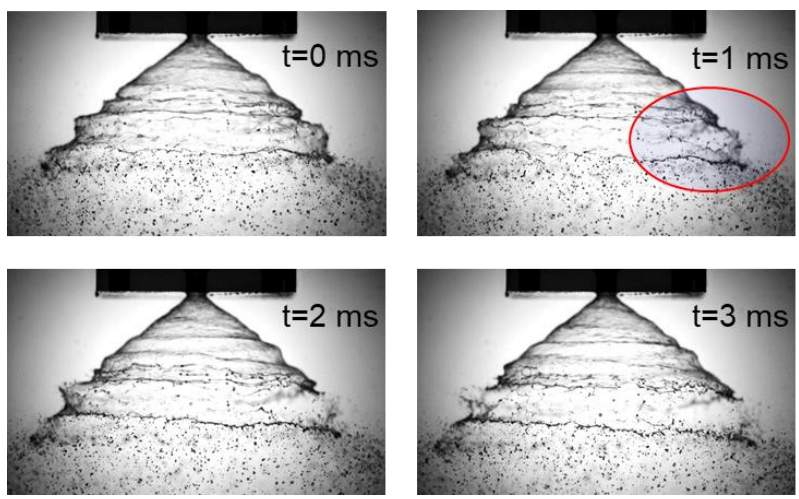

Fig. 4.8 Spray front images when breakup of ligament occurred

The summary of this breakup process for the liquid swirl injector could be visualized as in Fig. 4.9. At first, the wavy sheet was formed by aerodynamic forces on a thin liquid sheet flow. The sheet then tore at the peak point of the wave. Because air flow can easily affect the sheet, this was the weakest point of the sheet. After that, detachment of ligament occurred, and via surface tension force, concentration of liquid occurred, and a pipe-shaped liquid ring formed. From the thin sheet layer, small droplets were also formed simultaneously. Finally, the pipe-shaped liquid was

converted to large droplets.

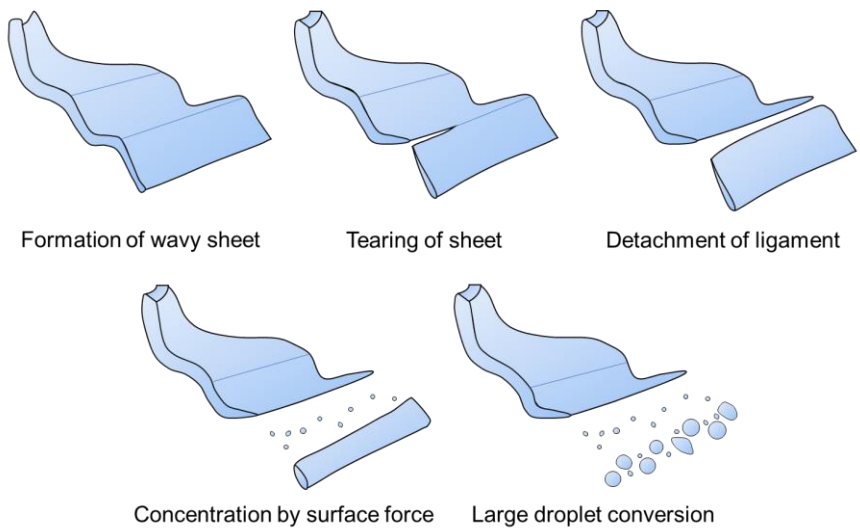

Fig. 4.9 Scheme of breakup process for liquid swirl injector

At this time, because of the rapid conversion of droplets and relatively long-term sheet progression, concentration of droplets was thought to have occurred. Therefore, droplet dispersion with respect to time was investigated. An intensity profile was obtained after the breakup, which is shown as the dotted line in Fig. 4.10. This intensity area could represent the region of droplets that passed through a certain area. This intensity profile is shown in Fig. 4.11 (a), and given an appropriate threshold, the region of water occupied by large droplets could be illustrated as in Fig. 4.11 (b).

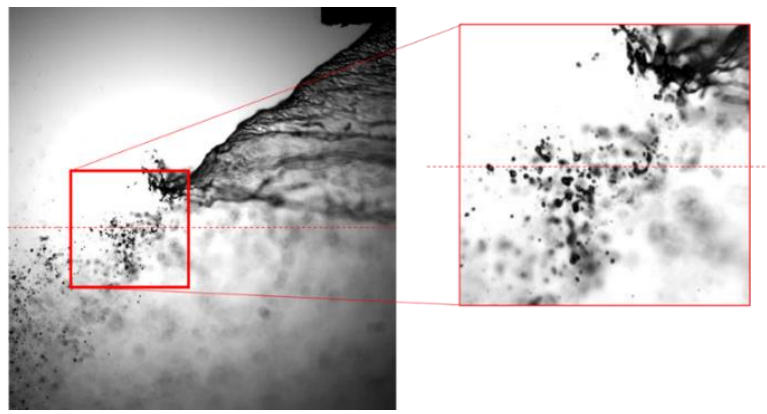

Fig. 4.10 Large droplets after detachment

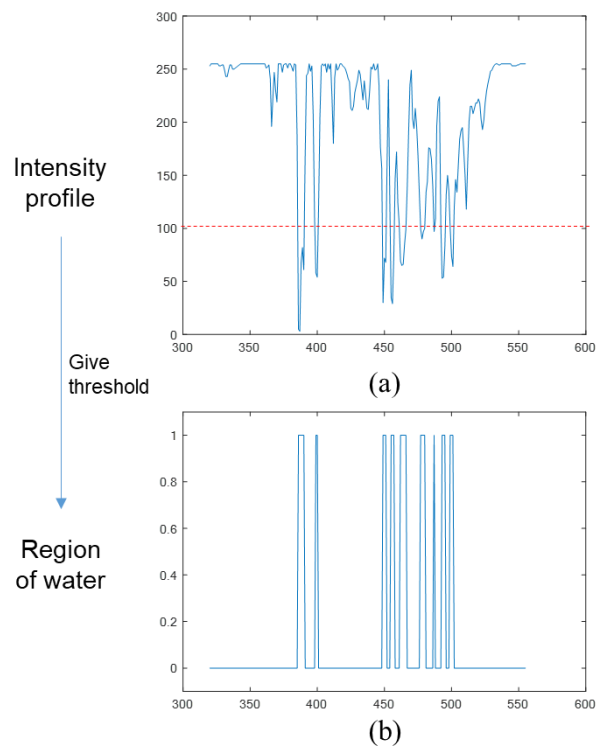

Fig. 4.11 (a) Intensity profile, and (b) region of water droplets from the intensity profile

Through this process, the portion of flow passing through a certain area could be measured. The frequency domain result was then obtained via FFT, as shown in Fig. 4.12. Although the amplitude was small, and low-frequency noise was also observed, the self-oscillation frequency, 312 Hz, was measured as expected. From the results, self-oscillation frequency can be said to affect the whole flow and breakup process for a liquid single swirl injector.

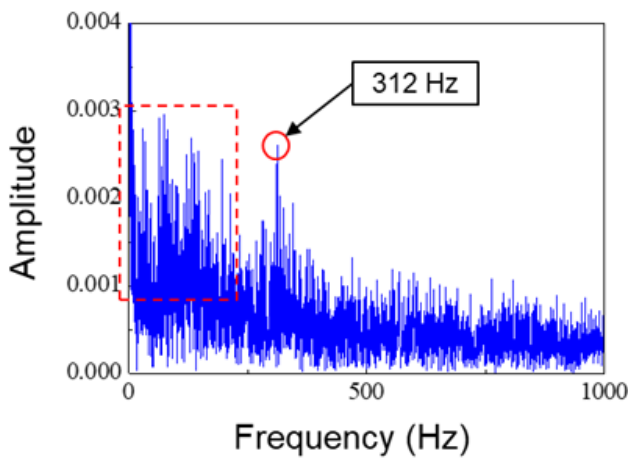

Fig. 4.12 FFT result for portion of area where large droplet passed through an area of interest

CHAPTER 5

RELATION BETWEEN SELF-OSCILLATION AND DYNAMIC CHARACTERISTICS OF SWIRL INJECTOR

5.1 Objectives and Test Conditions

As shown in Chapter 3, and Chapter 4, self-oscillation instability greatly affected static characteristics of swirl injector. In Chapter 5, the effect of self-oscillation instability on dynamic characteristics of swirl injector was examined. Normally, dynamic characteristics was mainly dealt with studies of injector dynamics. However, injector dynamics studies have been focused mainly on instability from the internal structure of the swirl injector. Studies about the effects of self-oscillation instability on the dynamic characteristics of an injector have been lacking. Therefore, in this chapter, the effects of self-oscillation on the actual atomization process and on the dynamic characteristics of swirl injector were examined experimentally. Furthermore, to determine the effect of self-oscillation frequency on the atomization process in a real environment, the process of sheet breakup and droplet formation in the presence of external pulsation was examined.

To compare the result of pulsation and non-pulsation case., the experimental condition was set same as Chapter 4. The geometry of the swirl injector in this

chapter was as follows: the swirl chamber length L_s was 19 mm, the swirl chamber diameter D_s was 18 mm, the orifice diameter D_o was 9 mm, the number N_t of tangential inlet ports was 3, and the tangential inlet port diameter D_t was 1 mm. The condition of the experiment was as follows: the injector pressure drop P_m was 3 atm, the mass flow rate $\dot{m}$ was 40.5 g/s, and the ambient pressure was fixed at 1 atm. From this condition, self-oscillation frequency was set at 312 Hz.

5.2 Dynamic Characteristics of Liquid Swirl Injector

To study the dynamic characteristic of the injector, the dynamic gain, which can be calculated from mass flow divided by input pressure, should be obtained with respect to frequency. However, real-time measurement of mass flow rate was difficult in the experiment. Instead, film thickness or air core diameter has been used to calculate the mass flow characteristic indirectly. According to Bazarov (1979) and Fu et al. (2010), flow rate q can be represented as Eq. (5.1).

$$q = \bar{q} + C_1 \xi, \tag{5.1}$$

where $\bar{q}$ is the mean flow rate, and C_1 is a constant.

That is, the mass flow rate fluctuation is proportional to the perturbation of the flow surface ξ in the swirl injector. In this study, the fluctuation amplitude of the air core diameter was measured from a backlit image of the internal flow, as shown in Fig. 5.1, for 1.66 s at 6000 frames per second, with the external pulsation frequency varied using a mechanical pulsator. The peak amplitude of the FFT result at each external pulsation frequency case was accumulated, as shown in Fig. 5.2. At this time, the fluctuation amplitude of the air core diameter was divided by the average air core diameter, 6.719 mm, to make it dimensionless. As a result, the peak frequency was measured to be near 312 Hz. This result seems to be related to the injector self-oscillation frequency shown in the previous Chapter 3, Chapter 4. Afterward, changes caused by external excitation on the spray characteristics were investigated.

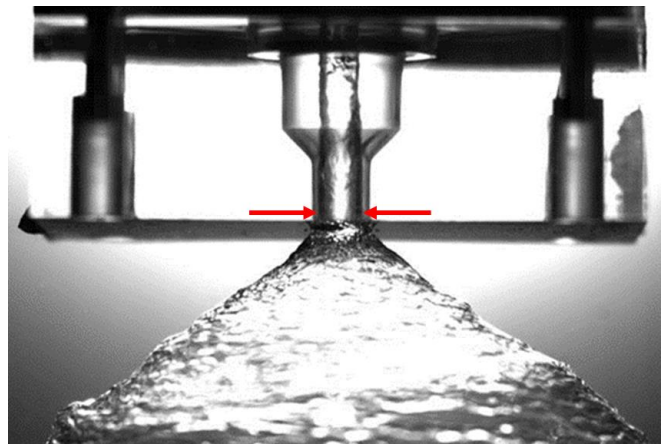

Fig. 5.1 Air core diameter measurement point at internal flow image of swirl injector

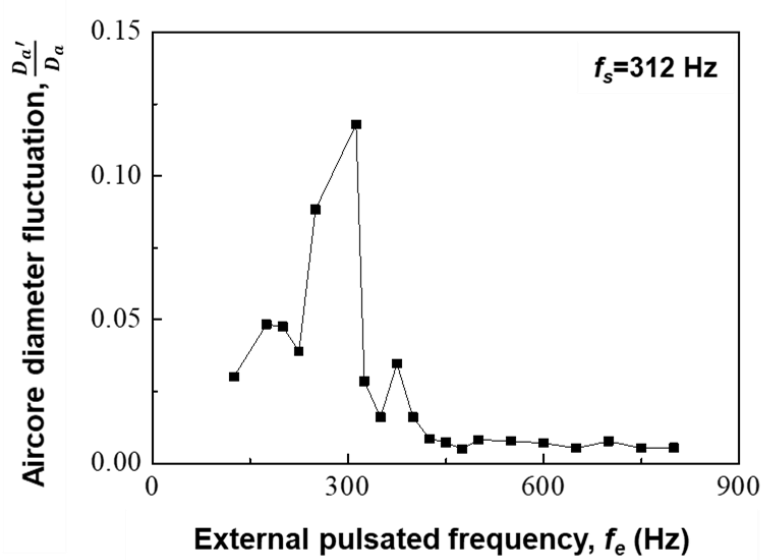

Fig. 5.2 Non-dimensional air core diameter fluctuation with respect to varying external pulsated frequency

5.3 Effect of External Pulsation with Self-oscillation Frequency

5.3.1 Effect of External Pulsation on Spray Angle

For comparison, external pulsations of 312 Hz and 350 Hz were applied for tuned and out of tune cases. Significant differences can be observed between two spray images with external pulsation, as shown in Fig. 5.3.

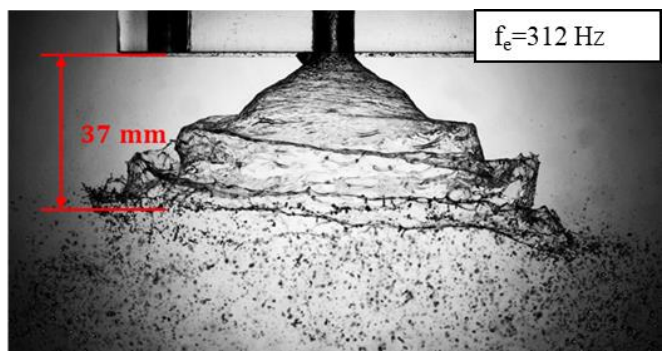

(a)

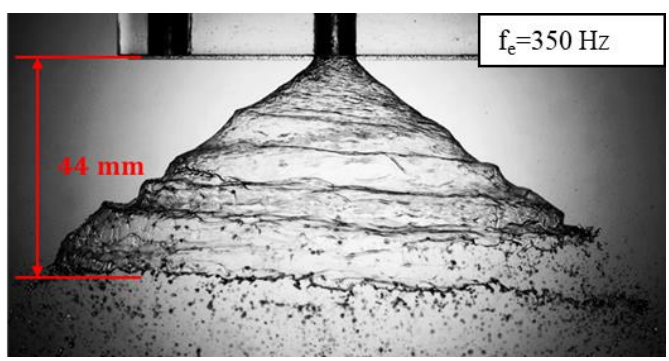

(b)

Fig. 5.3 External spray images with pulsation of (a) 312 Hz and (b) 350 Hz cases

First, the mean breakup length observed in the tuned case is 37 mm, which is about 20% shorter than the mean breakup length in out of tune case, which is 44 mm. The breakup length is one of the important factors determining the size of the combustion chamber. If the breakup length is greater than the design value, there is a problem that the spray or flame reaches the wall of the combustion chamber; and if the breakup length is shorter than the designed value, it becomes difficult to mix the propellant sufficiently (Lefebvre, 1989). According to the results of this study, it can be observed that the breakup length can be changed even when the structure and pressure difference are the same.

Furthermore, the strength of the fluctuation was high in the tuned case. Figure 5.4 shows the FFT results of external spray angle with external perturbation for tuned and out of tune cases. Figure 5.4 (a) shows only one peak frequency at 312 Hz for the tuned case, and Fig. 5.4 (b) shows two peak frequencies, the self-oscillation frequency at 312 Hz and the applied frequency at 350 Hz, for the out of tune case. In the out of tune case, the FFT amplitude, which means the strength of the fluctuation, at 312 Hz was 0.766° and the FFT amplitude at 350 Hz was 0.661°. However, when these two perturbation strengths were applied with the same frequency, the FFT amplitude changed to 2.867°, which was 2.01 times higher than the simple addition of natural and applied amplitudes. When the spray angle fluctuation increases, the engine efficiency can decrease because some of the propellants reach the combustion chamber wall. To solve this problem, it is not only necessary to design an injector with low fluctuation amplitude, but it is also

important to check the frequency band of external sources and avoid this frequency band by considering the self-oscillation of injector.

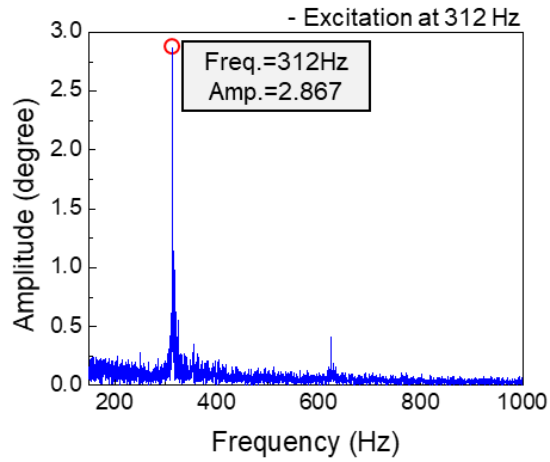

(a)

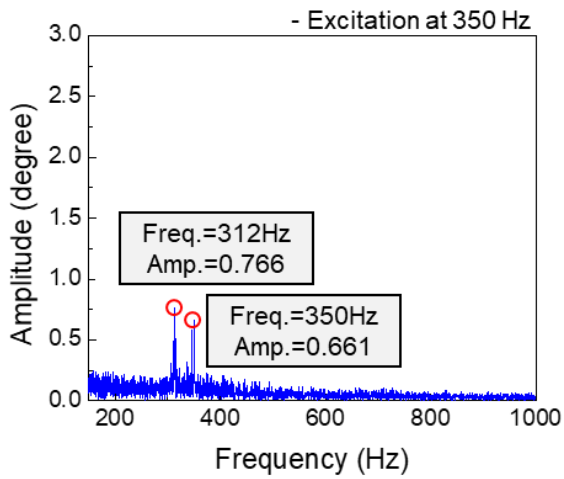

(b)

Fig. 5.4 FFT results of external spray angle with external pulsation for (a) 312 Hz and (b) 350 Hz case

5.3.2 Effect of External Pulsation on Liquid Sheet Characteristics

Sheet wave amplitudes were measured for five positions from 1.8 mm to 15.2 mm with 3.6 mm intervals which were same detection points with Chapter 4. As shown in Fig. 5.5, the case of excitation frequency with 312 Hz which was injector's self-oscillation frequency was found to have the largest wave fluctuation amplitude.

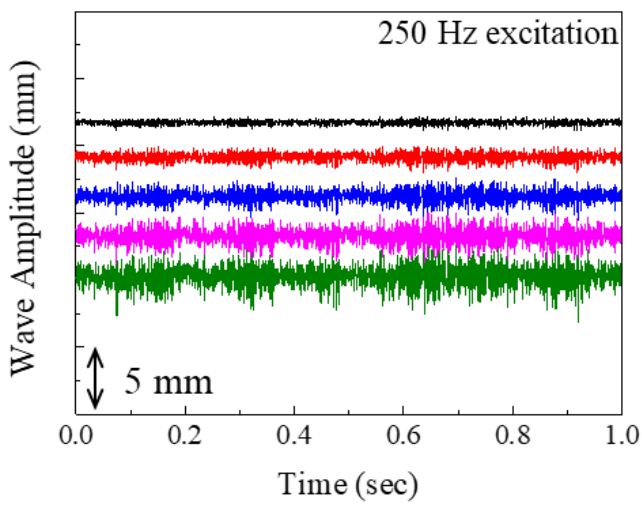

(a)

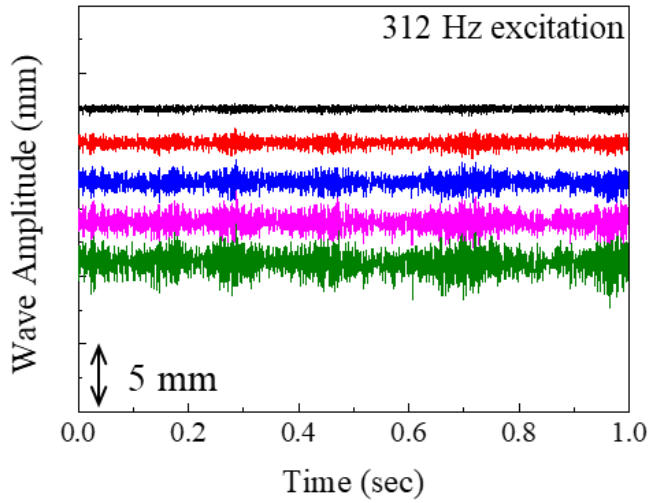

(b)

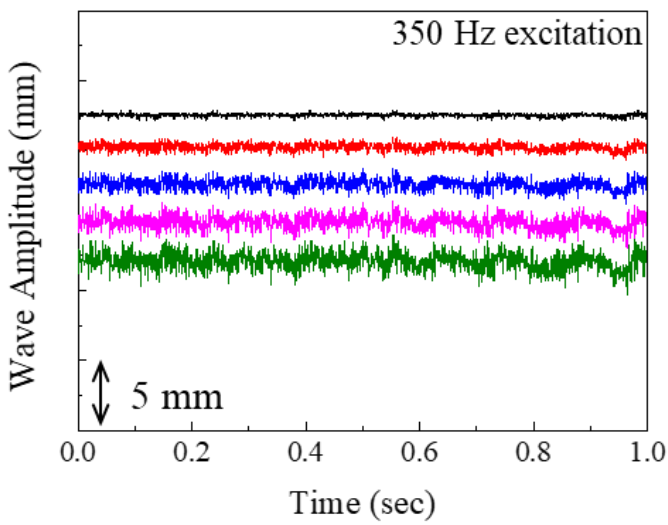

(c)

Fig. 5.5 Sheet wave fluctuation amplitude with (a) 250 Hz, (b) 312 Hz, and (c) 350 Hz excitation

It can be seen more clearly in Fig. 5.6, which was the result of FFT at 15.2 mm case. In all cases, 312 Hz peak, which was the injector self-instability frequency, was detected. The excitation frequency was also detected for 250 Hz and 350 Hz excitation cases. However, large amplitude peak was observed for the 312 Hz excitation, similar to FFT result of spray angle at previous chapter. From the results, it was shown that even though external pulsation could change characteristic of external spray wave, effect of self-oscillation on wave amplitude strongly remained. Moreover, by applying external pulsation with same frequency as self-oscillation, drastic increase of wave amplitude could be generated.

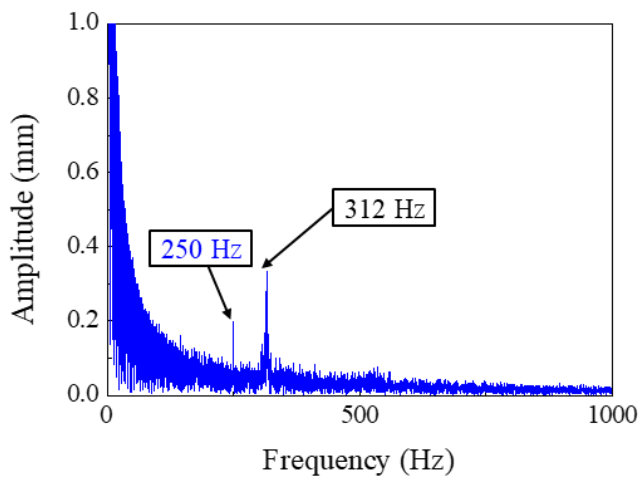

(a)

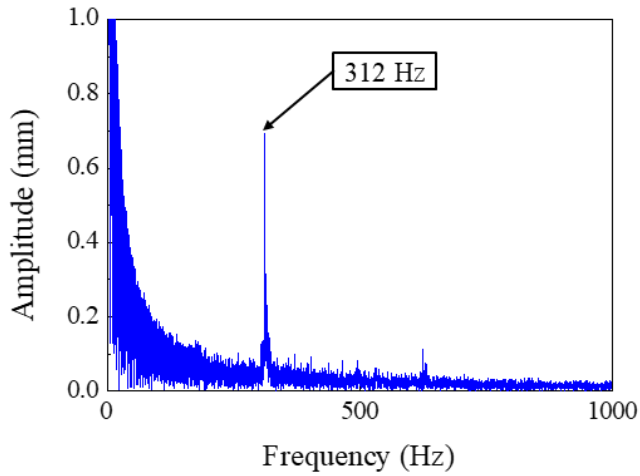

(b)

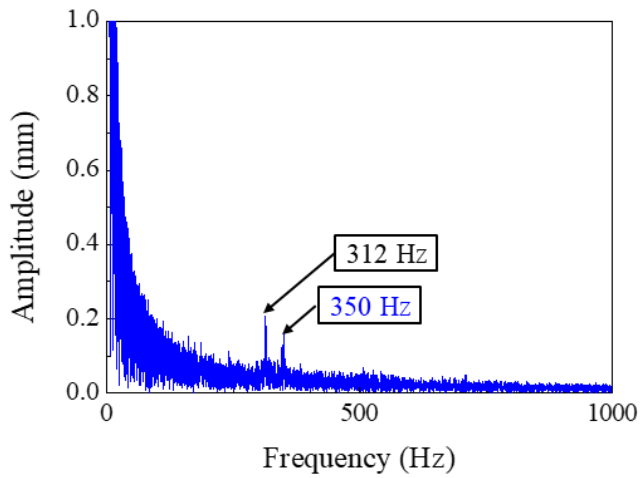

(c)

Fig. 5.6 FFT result of sheet wave with (a) 250 Hz, (b) 312 Hz, and (c) 350 Hz excitation

5.3.3 Effect of External Pulsation on Liquid Sheet Characteristics

Characteristics of breakup length according to the excitation frequency was investigated. As a result, when the injector self-oscillation frequency and the external pulsation frequency were different, it was confirmed that the breakup period could be either inverse of the external pulsation frequency or inverse of injector self-oscillation frequency. As shown in Fig. 5.7 (a), the interval between breakups was 0.004 s (=1/250 Hz) in measurement time at 0 to 0.02 seconds. Whereas, at the measurement time at 0.02 to 0.04 seconds, the interval between breakups was 0.003 s, which was the inverse of the injector self-oscillation frequency, 312 Hz. This phenomenon occurred because the amplitude of the excitation and self-instability on the sheet was similar, as shown in Fig. 5.6 (a). Period of breakup seemed to be changed according to the greater influence of the two instability factors at that time interval. On the other hands, when pulsation with the same frequency of self-oscillation was applied, the interval between breakup was constant value, 0.003 s, same as Fig. 4.6 in Chapter 4.

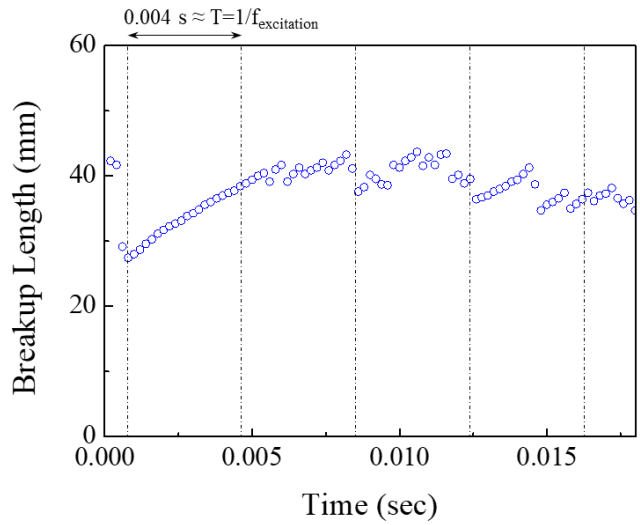

(a)

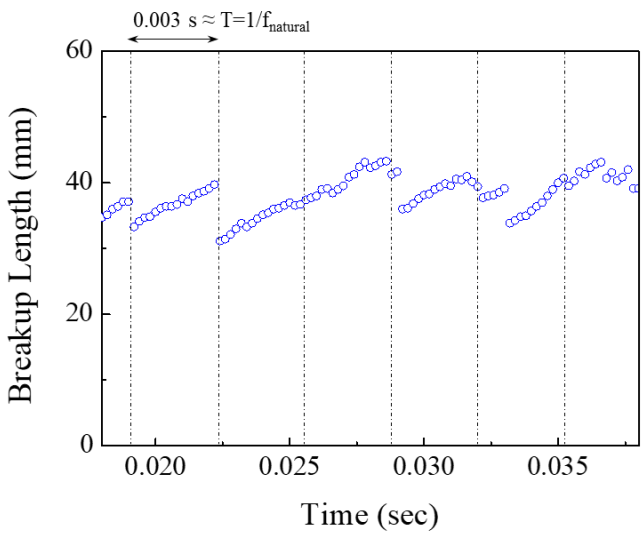

(b)

Fig. 5.7 Breakup length with 250 Hz pulsation case at (a) 0 to 0.02 s (b) 0.02 to 0.04 s

Figure 5.8 shows ligament breakup process with pulsation. The breakup process was similar with non-pulsation case, but it was shown that ligament to droplets conversion took longer than non-pulsation case. As shown in Fig. 5.8, ligament fully converted to droplets about 2 ms after detachment of ligament occurred. This seems to be due to the difference in thickness of each ligament. Figure 5.9 shows the difference of ligament to droplet conversion process with and without external pulsation. With pulsation, sheet could be detached before it becomes thin enough due to the pulsation energy. Therefore, respectively thick ligament formed and detachment take a longer time.

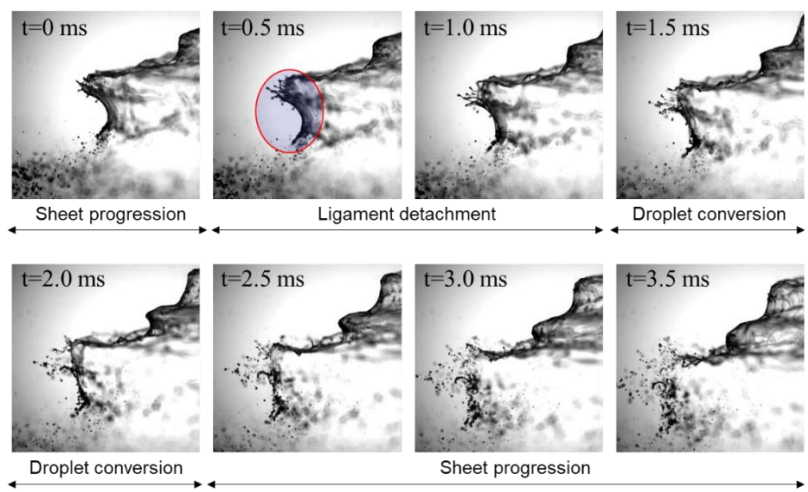

Fig. 5.8 Ligament detachment process with 312 Hz pulsation

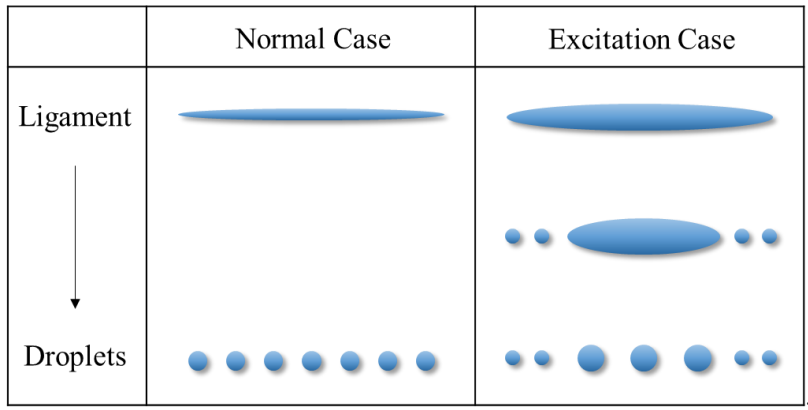

Fig. 5.9 Scheme of ligament to droplet conversion process with and without excitation

5.4 Comparison of Characteristics with and without External Pulsation

The average breakup length was obtained with respect to varying external pulsated frequency, from 100 to 500 Hz. At this time, breakup lengths measured from 10000 images taken for 1.66 s at 6000 frames per second, were averaged to obtain a precise value. The result is shown in Fig. 5.10. In this graph, the breakup length for the non-pulsated case was used as the 0 Hz external pulsated frequency case value. The minimum value of breakup length was observed near the 312 Hz external pulsated frequency. The tendency of breakup length with respect to external pulsated frequency was similar to the inverse of the air core diameter fluctuation tendency shown in Fig. 5.2 at Chapter 5.2. According to Jazayeri and Li (2000), as initial disturbance amplitude increases, the liquid sheet breaks up at earlier times. In this experiment, because of the large fluctuation amplitude of the air core diameter with 312 Hz external pulsation, the spray sheet had a high initial wave fluctuation amplitude, and breakup occurred earlier.

To investigate the characteristics of breakup with respect to pulsation in more detail, the wave characteristics of the sheet were observed from external sheet flow images. As shown in Fig. 5.11, the boundary of the sheet was taken through a gradient image obtained using the MATLAB program.

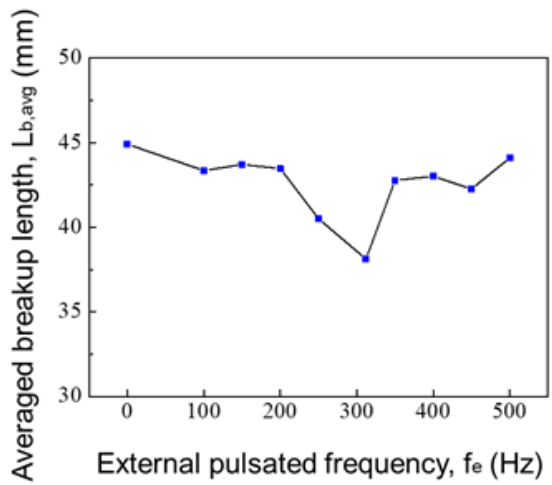

Fig. 5.10 Average breakup length with respect to varying external pulsated frequency

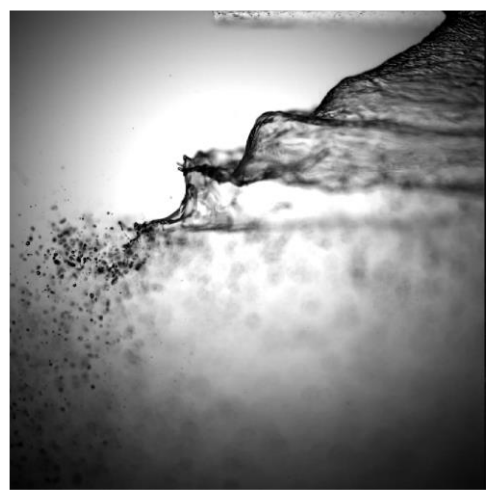

(a)

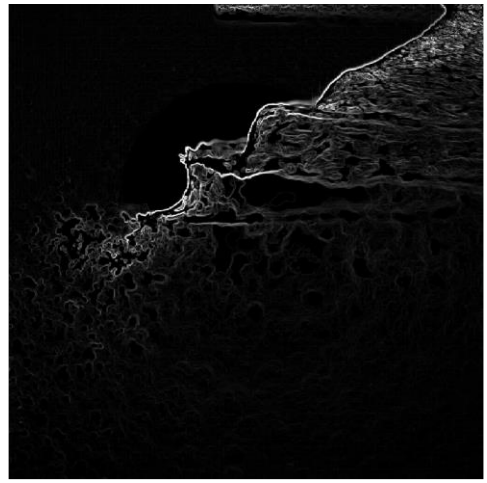

(b)

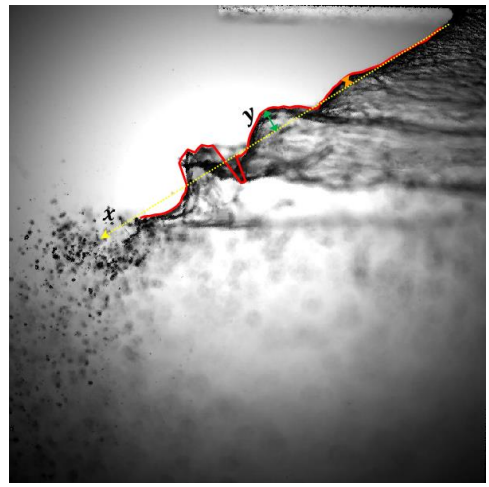

(c)

Fig. 5.11 (a) Raw image, (b) gradient image, and (c) resulting image with edge line

At this time, the displacement y of the wave with respect to sheet propagation distance x was measured from images taken for 1.66 s at 6000 frames per second. Through the use of the root mean square (RMS) deviation of the distance y, the fluctuation amplitude T was obtained with respect to sheet propagation distance x, as shown in Fig. 5.12. Given the breakup length for each case and the spray half-angle, the sheet propagation distance x_b at breakup, which is indicated as the red dashed line in Fig. 5.12, could be calculated. In linear theory, $\ln(T_b/T_0)$ is an important factor in predicting the breakup characteristic. It should be measured experimentally and has an almost constant value of 12 for a plane liquid sheet (Dombrowski and Johns, 1963). However, the value of $\ln(T_b/T_0)$ was not the same for the swirl injector case. Kim et al. (2007) experimentally calculated $\ln(T_b/T_0)$, and a smaller value of $\ln(T_b/T_0)$, 6.9, was obtained. They concluded that it was due to the swirling effect, which made the liquid sheet break up easily. In this study for the non-pulsation case, the value of $\ln(T_b/T_0)$ was 4.63. On the other hand, with external pulsation, a smaller value of $\ln(T_b/T_0)$, 4.13, was measured, as shown in Fig. 5.12 (b) and (c). A major difference in the wave amplitude characteristic was the required time for breakup. When external pulsation was applied at a frequency equal to the self-oscillation frequency, 312 Hz, wave fluctuation amplitude increased faster with respect to sheet propagation distance than in other conditions. As a result, the minimum breakup length was observed at the 312 Hz external pulsation case.

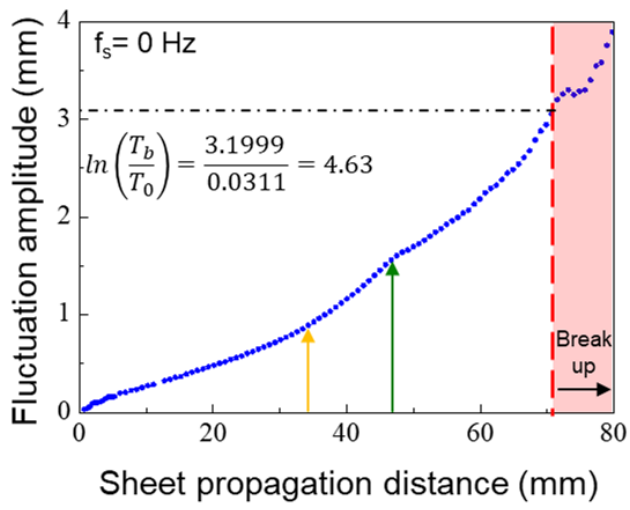
f_s= 0 Hz
ln(T_b/T_0) = 3.1999/0.0311 = 4.63
Break up
Fluctuation amplitude (mm)
Sheet propagation distance (mm)
0
1
2
3
4
0
20
40
60
80

(a)

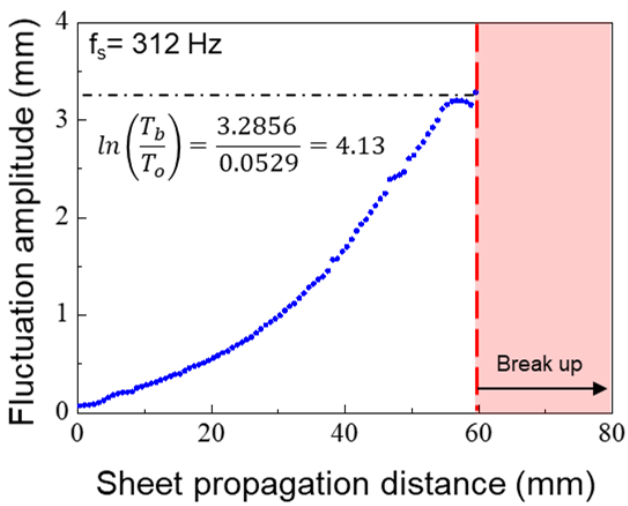
f_s= 312 Hz
ln(T_b/T_o) = 3.2856/0.0529 = 4.13
Break up
Fluctuation amplitude (mm)
Sheet propagation distance (mm)
0
1
2
3
4
0
20
40
60
80

(b)

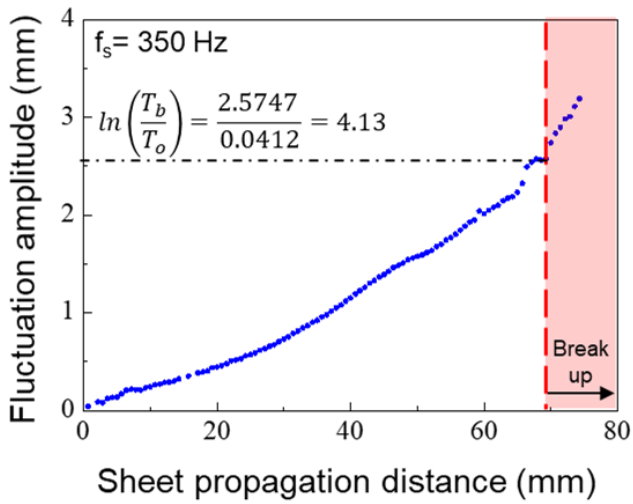

(c)

Fig. 5.12 Wave fluctuation amplitude with respect to sheet propagation distance for (a) non-pulsation, (b) 312 Hz pulsation, (c) and 350 Hz pulsation cases

The droplet diameters with and without pulsation were then compared. As described in Chapter 2.1, measurement of droplets was performed at 60 mm below the injector tip. The measured values of D_{10} and *SMD* are outlined in Table 5.1. When the cases with and without pulsation were compared, both D_{10} and *SMD* could be seen to become smaller when external pulsation applied, because of the energy from the pulsation. When the pulsation cases were compared, D_{10} had similar values in both the 312 Hz and 350 external pulsation cases. However, a higher *SMD* was measured when 312 Hz frequency external pulsation, which was the injector self-oscillation frequency, was applied, because both large and small droplets were increased by the periodic strong vibration.

Table 5.1 D_{10} and *SMD* with test conditions

	Non-pulsation case	Pulsation case	
		f_e = 312 Hz	f_e = 350 Hz
D_{10} (μm)	117.74	105.02	105.74
SMD (μm)	465.21	453.75	440.10

To verify this inference, the droplet distributions for each case were examined. The number of droplets with respect to droplet size, in 100 μm range intervals, were measured and divided by the total droplet number to determine the droplet distribution probability. The results are shown in Fig. 5.13. For the 312 Hz pulsation case, the proportion of droplets smaller than 100 μm was confirmed to be larger than for the 350 Hz pulsation case. At the same time, the proportion of droplets larger than 500 μm was also larger than for the 350 Hz pulsation case. This confirmed that the cause of large *SMD* value at the 312 Hz pulsation case was the non-uniform distribution of droplets owing to the periodic excitation.

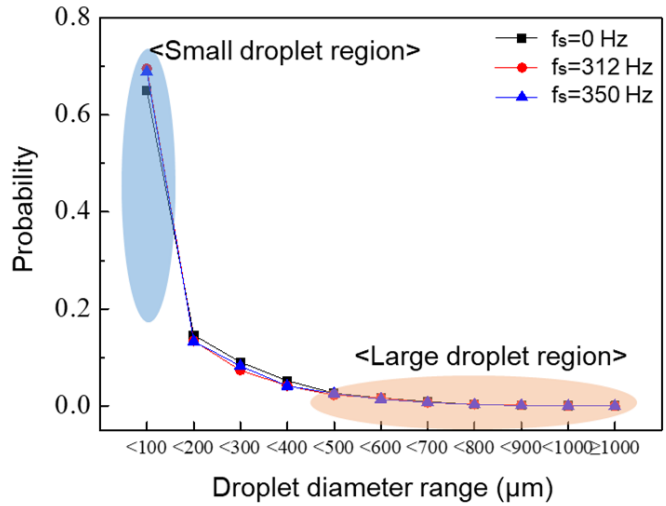

(a)

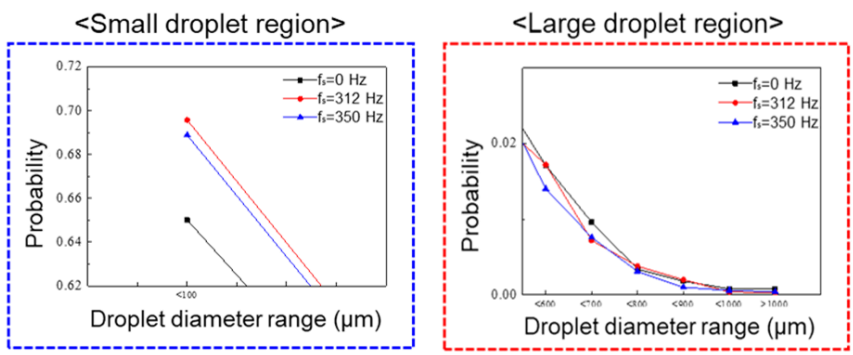

(b) (c)

Fig. 5.13 (a) Droplet distribution with respect to different pulsation conditions, (b) at small droplet region, and (c) large droplet region

CHAPTER 6

CONCLUSION

In this study, injector self-oscillation instability was investigated in the closed-type liquid single swirl injector. The dynamic characteristics was measured from internal and external flow. Effect of external pulsation on instability characteristic was then found. The summary of the study is as follows.

First, the characteristics of self-oscillation instability was found from internal flow image of swirl injector. From backlit image of the swirl injector which was made by transparent acrylic material, air core diameter could be detected. Fluctuation amplitude of air core diameter which represent dynamic gain of instability was then found from high speed camera image with 6000 frame per second. Fluctuation frequency of air core diameter which represent dynamic frequency of instability was also found from FFT result of time domain air core diameter. From these results, it was found that the amplitude of self-oscillation was inversely proportional to mass flow rate and self-oscillation frequency was proportional to mass flow rate. To find the characteristics of self-oscillation frequency in more detail, experiments with various swirl injector geometry was done. As a result, it was found that amplitude of self-oscillation was related to liquid momentum. When liquid momentum was increased by increasing mass flow rate or increasing swirl strength, the flow became more robust to external perturbation and instability amplitude decreased. On the

other hands, it was found that frequency of self-oscillation was related to liquid axial velocity at the orifice. This phenomenon was same as Kelvin Helmholtz instability. K-H instability is occurred by velocity difference with two phase flow at the shear layer and with velocity difference increase, instability frequency also increases. Relation of frequency and velocity could be represented from Strouhal number, and in this study, constant Strouhal number, 0.236 was found in all experiment cases.

Second, the effect of self-oscillation on swirl injector flow was investigated. Instability frequency of external flow was measured from spray angle. From the external images at 6000 frame per second, time domain spray angle was measured. FFT was then performed to acquire self-oscillation frequency at the external flow. As a result, it was found that the phenomenon of instability at external spray angle and internal air core diameter was same. The effect of the self-oscillation on external spray then investigated in more detail. At first, wave characteristic with sheet propagation was investigated from spray images. It was found self-oscillation frequency remained same with spray flow progression, and fluctuation amplitude was only increased. Effect of self-oscillation on breakup process was then examined. In this time, it was confirmed that breakup occurred periodically, which have period same as inverse of self-oscillation frequency. Moreover, spending time between sheet progress and droplet conversion was different. Due to this difference, periodical concentration of droplet flow was formed. In summary, self-oscillation instability of swirl injector had effect on whole process of injector flow, from internal to breakup.

Finally, the effect of external pulsation on swirl injector flow and the relation between injector dynamic characteristic and self-oscillation instability was investigated. At this time, specific frequency could be applied at the feed line by using the hydraulic mechanical pulsator. Experimental condition which had 312 Hz self-oscillation frequency was used for this investigation. At first, dynamic gain was measured from air core diameter with respect to frequency, and the maximum gain found at the frequency same as self-oscillation frequency. Breakup length with respect to excitation frequency was then measured. In this case, breakup length was minimum at the frequency same as self-oscillation frequency due to the high wave fluctuation. From the result, the fluctuation amplitude and breakup length were determined to be inversely related, and self-oscillation frequency was inferred to have some role on the dynamic characteristic of breakup length. Both the mean drop size and the SMD were smaller than those without pulsation. In addition, when the pulsation was performed at the injector self-instability frequency, an unusual phenomenon occurred for the SMD. The SMD was confirmed to become larger when excitation was performed at the injector self-instability frequency. This tendency seems to be due to the non-uniform distribution of droplets in the case of self-instability frequency pulsation.

In conclusion, through this study, experimental data on the self-oscillation phenomenon of a single liquid swirl injector were obtained. Furthermore, the manifestation of unstable spray characteristics, when nonlinear large pulsation was applied, was experimentally confirmed. Self-oscillation with external pulsation was

also confirmed to possibly change the characteristics of injector, especially breakup length and SMD, which is a combustion-related factor. Therefore, knowledge of self-oscillation instability frequency of injector is important for engine system design. Furthermore, frequency of pressure noise from feed system should be confirmed before entire engine system combining to prevent engine failure. Additionally, further research may be needed to clarify the relationship between self-instability, SMD, and combustion through an actual combustion test in the presence of such an instability.

REFERENCES

Ahn, K., Choi, H. S., "Combustion Dynamics of Swirl Coaxial Injectors in Fuel-rich Combustion," *Journal of Propulsion and Power*, Vol. 28, No. 6, 2012, pp. 1359-1367.

Anderson, W. E., Miller, K. L., Ryan, H. M., Pal, S., Santoro, R. J., "Effect of Periodic Atomization on Combustion Instability in Liquid-Fueled Propulsion Systems," *Journal of Propulsion and Power*, Vol. 14, No. 5, 1998, pp. 818-825.

Bayvel, L., Orzechowski, Z., "*Liquid Atomization*," Philadelphia, Taylor and Francis, 1993.

Bazarov, V. G., "*Liquid Injector Dynamics*," Mashinostroenie, Moscow, 1979.

Bazarov, V. G., Yang, V., "Liquid-propellant Rocket Engine Injector Dynamics," *Journal of Propulsion and Power*, Vol. 14, No. 5, 1998, pp. 797-806.

Bazarov, V., Lee, E., Lineberry, D., Swanner, B., Frederick, R., "Pulsator Designs for Liquid Rocket Injector Research," *In 43rd AIAA/ASME/SAE/ASEE Joint Propulsion Conference & Exhibit*, AIAA 2007-5156, July 2007.

Chen, X., Yang, V., "Effect of Ambient Pressure on Liquid Swirl Injector Flow Dynamics," *Physics of Fluids*, Vol. 26, No. 10, 2014, p. 102104.

Chung, Y., Kim, H., Jeong, S., Yoon, Y., "Dynamic Characteristics of Open-Type Swirl Injector with Varying Geometry," Journal of Propulsion and Power, Vol. 32, No. 1, 2016, pp. 583-591.

Dasgupta, D., Nath, S., Mukhopadhyay, A., "Linear and non-linear analysis of breakup of liquid sheets: a review," *Journal of the Indian Institute of Science*, Vol. 99, No. 1, 2019, pp. 59-75.

Dombrowski, N., Johns, W. R., "The Aerodynamic Instability and Disintegration of Viscous Liquid Sheets," *Chemical Engineering Science*, Vol. 18, No. 3, 1963, pp. 203-214.

Eberhart, Chad. J., Frederick, Jr., Robert A., "Fluid Pulsations of a Swirll Coaxial

Injector Under High-Frequency Self-oscillation," *Journal of Propulsion and Power*, Vol. 33, No. 4, 2017, pp. 804-814.

Fraser, R.P., Eisenkam, P., Dombrowski, N., Hasson, D., "Drop formation from rapidly moving liquid sheets," *American Institute of Chemical Engineers*, Vol. 8, No. 5, 1962, pp. 672-680.

Fu, Q. F., Yang, L. J., Wang, X. D. "Theoretical and Experimental Study of the Dynamics of a Liquid Swirl Injector," *Journal of Propulsion and Power*, Vol. 26, No. 1, 2010, pp. 94-101.

Im, J., Kim, D., Han, P., Yoon, Y., Bazarov, V., "Self-oscillation Characteristics of a Gas-liquid Swirl Coaxial Injector," *Atomization and Sprays*, Vol. 19, No. 1, 2009, pp. 57-74.

Ismailov, M., Heister, S. D., "Dynamic Response of Rocket Swirl Injectors, Part I: Wave Reflection and Resonance," *Journal of Propulsion and Power*, Vol. 27, No. 2, 2011a, pp. 402-411.

Ismailov, M., Heister, S. D., "Dynamic Response of Rocket Swirl Injectors, Part II: Nonlinear Dynamic Response," *Journal of Propulsion and Power*, Vol. 27, No. 2, 2011b, pp. 412-421.

Jazayeri, A., Li, X., "Nonlinear instability of plane liquid sheets," *Journal of Fluid Mechanics*, Vol. 406, 2000, pp. 281-308.

Kang, Z., Li, X., Mao, X., "Experimental investigation on the surface wave characteristics of conical liquid film," *Acta Astronautica*, Vol. 149 ,2018, pp. 15-24.

Kenny, R. J., Hulka, J. R., Moser, M. D., Rhys, N. O., "Effect of Chamber Backpressure on Swirl Injector Fluid Mechanics," *Journal of Propulsion and Power*, Vol. 25, No. 4, 2009, pp. 902-913.

Khil, T., Chung, Y., Bazarov, V. G., Yoon, Y., "Dynamic Characteristics of Simplex Swirl Injector in Low Frequency Range," *Journal of Propulsion and Power*, Vol. 28, No. 2, 2012, pp. 323-333.

Kim, D. Im, J., Koh, H., Yoon, Y., "Effect of ambient gas density on spray

characteristics of swirling liquid sheets, *Journal of Propulsion and Power*, Vol. 23, No. 3, 2007, pp. 603-611.

Kim, S., Khil, T., Kim, D., Yoon, Y., "Effect of Geometric Parameters on the Liquid Film Thickness and Air Core Formation in a Swirl Injector," *Measurement Science and Technology*, Vol. 20, No. 1, 2008, p. 015403.

Lefebvre, A.H., "*Atomization and Sprays*," Hemisphere, New York, 1989.

Liao, Y., Sakman, A. T., Jeng, S. M., Jog, M. A., Benjamin, M. A., "A comprehensive model to predict simplex atomizer performance," *Journal of Engineering for Gas Turbines Power*, Vol. 121, 1999, pp. 285-294.

Lienemann, H., Shrimpton, J., Fernandes, E., "A Study on the Aerodynamic Instability of Attenuating Liquid Sheets," *Experiments in fluids*, Vol. 42, No. 2, 2007, pp. 241-258.

Panchagnula, M. V., Sojka, P. E., Santangelo, P. J., "On the three-dimensional instability of a swirling, annular, inviscid liquid sheet subject to unequal gas velocities," *Physics of Fluids*, Vol. 8, 1996, pp. 3300-3312.

Rangel, R. H., Sirignano, W. A., "The linear and nonlinear shear instability of a fluid sheet," *Physics of Fluids*, Vol. 3, 1991, pp. 2392-2400.

Squire, H. B., "Investigation of the instability of a moving liquid film," *British Journal of Applied Physics*, Vol. 4, 1953, pp, 167-169.

Wilson, M., Lineberry, D., Moser, M., "Experimental Pulsator Characterization for Liquid Injector Research," In 45th AIAA/ASME/SAE/ASEE Joint Propulsion Conference & Exhibit, AIAA 2009-5491, August 2009.

Yang, A., Yang, S., Xu, Y., Li, L., "Periodic Atomization Characteristics of Simplex Swirl Injector Induced by Klystron Effect," Chinese Journal of Aeronautics, Vol. 31, No. 5, 2018, pp. 1066-1074.

초 록

분사기는 액체를 미립화 시키는 장치로, 연소, 농업, 냉각 등 다양한 분야에서 사용되어 왔다. 분사기는 분무 방식에 따라 스월형, 스크류형, 충돌형, 전단형, 핀틀형 등 다양하게 분류되며, 그 중 폐쇄형 스월 분사기의 경우 구조가 간단하고 성능이 우수하기 때문에 러시아를 중심으로 로켓 엔진 분사기로서도 널리 사용되어 왔다. 하지만 분사기가 연소에 사용되는 경우에는 연소 불안정과의 관계로 인해 분사기의 유동 불안정성이 중요해진다. 연소 불안정은 연소실의 음향 특성과 열 방출 특성이 서로 결합하면서 발생하며, 이 때 열 방출 특성은 유동 특성에 따라 변경된다. 분사기로부터의 추진제 공급이 불완전하거나 추진제의 미립화가 불규칙하게 되면, 균일한 열 방출이 발생하지 못하며 연소 불안정이 발생하기 쉬워진다. 따라서 주기적으로 액체 입자 분포나 분무 안정성과 같은 분사기 유동의 동적 특성을 살펴봐야 한다. 따라서 본 연구에서는 다양한 실험 조건에 따라 내부 유동 특성을 측정하여 분사기의 자체 불안정 특성을 살펴보았다. 그리고 자체 불안정이 스월 분사기 외부 유동에 미치는 영향을 살펴보았다. 마지막으로, 스월 분사기의 동적 특성에 대한 자체 불안정과의 연관성을 살펴보기 위해 외부 가진을 적용하였을 때의 유동 특성을 살펴보았다. 실험 결과는 다음과 같다.

먼저, 분사기 자체 불안정 특성은 스월 분사기의 내부 유동 이미지로 부터 살펴보았다. 이로부터 자체 불안정의 진폭은 유량에 반비례하고 주파수는 유량에 비례함을 발견하였다. 자체 불안정의 특성을 더 자세히 살펴보기 위해 다양한 구조의 스월 분사기 형상을 사용하여 실험을 수행하였다. 그 결과, 자체 불안정 진폭은 액체의 운동량과 관련된 것으로 밝혀졌다. 한편, 자체 불안정의 주파수는 오리피스에서의 축방향 유동 속도와 관련된 것으로 밝혀졌다. 이 현상은 Kelvin-Helmholtz 현상과 유사한 것으로 확인되었다. 주파수와 축방향 속도의 관계는 Strouhal 수로 나타낼 수 있으며, 본 연구에서는 모든 실험 사례에서 0.236의 거의 일정한 Strouhal 수가 관찰되었다.

다음으로, 자체 불안정이 스월 분사기 유동에 미치는 영향을 살펴보았다. 외부 분무각 및 내부 에어 코어 직경에서의 불안정을 살펴본 결과 각각의 불안정 특성이 동일함이 밝혀졌다. 그리고 외부 유동에 대한 자체 불안정의 영향의 경우, 우선, 파동 형태의 액막 특성을 외부 유동 이미지로부터 살펴보았다. 자체 불안정 주파수는 유동이 진행하더라도 동일하게 유지되었고 불안정의 진폭만 증가하였다. 액막 분열 과정에서 자체 불안정의 영향을 살펴본 결과 주기적으로 액막 분열이 발생함을 확인할 수 있었는데, 분열 주기는 자체 불안정 주파수의 역수와 같음을 확인하였다. 또한, 액막 진행과 액적으로의 변환 사이의 소요되는 시간이 달

라 주기적으로 액적 분포의 밀집 현상이 나타남을 확인하였다. 이를 통해 분사기 자체 불안정이 분사기 내부 유동부터, 액막 형성, 분열, 그리고 액적 형성에 까지 전반적인 영향을 미치고 있음을 확인할 수 있었다.

마지막으로, 스월 분사기 유동에 대한 외부 가진의 영향 및 인젝터 동특성과 자체 불안정 간의 관계에 대해 살펴보았다. 이때 기계식 가진기를 사용하여 공급 라인에 특정 주파수의 압력 섭동을 가하였다. 실험에는 312Hz의 자체 불안정 주파수를 가지는 분사기 형상 및 실험 조건이 사용되었다. 주파수에 대한 에어 코어 직경으로부터 동특성을 살펴본 결과, 자체 불안정 주파수와 동일한 주파수에서 에어 코어 섭동이 가장 크게 발생함을 확인할 수 있었다. 그리고 가진 주파수에 대한 스월 분사기의 액막 분열 길이를 측정한 결과, 액막 분열 길이는 자체 불안정 주파수와 동일한 주파수의 가진을 가할 때 가장 빠르게 분열함을 확인할 수 있었다. 즉. 자체 불안정성 주파수는 분열 길이의 동특성에 중요한 역할을 함을 확인하였다. 평균 액적 크기와 SMD는 외부 가진이 있을 경우 더 작게 나타났고, 가진이 있는 경우 중에서도 인젝터 자체 불안정성 주파수와 동일한 주파수의 가진이 있는 경우, 그 이외 주파수로 가진한 경우에 비해 더 큰 SMD를 가짐을 확인하였다. 이는 자체 불안정 주파수 가진을 가했을 때는 액적 분포가 더 불균일해지기 때문으로 확인되었다.

결론적으로, 본 연구를 통해 액체 스월분사기의 자체 불안정 현상에

대한 실험 데이터를 얻었다. 또한, 큰 섭동이 있는 경우의 불안정한 분무 특성이 실험적으로 확인되었다. 자체 불안정 주파수를 가지는 외부 가진이 있는 경우 분열 길이나 SMD 같은 연소와 관련된 분무 특성에 영향을 미침을 확인하였다. 따라서 분사기의 자체 불안정 주파수에 대한 지식은 엔진 시스템 설계에 중요하다. 특히, 엔진에 발생하는 문제를 방지하기 위해 전체 엔진 시스템을 결합하기 전에 공급 시스템에서의 노이즈 주파수 확인이 중요함을 확인할 수 있었다. 추가적으로, 이러한 불안정성이 존재하는 경우 실제 연소 시험을 통해 자기 불안정성, SMD 및 연소 사이의 관계를 명확하게 하는 연구가 수행된다면 인젝터 동역학에서 중시하는 분사기를 통한 연소 불안정 제어에 한발짝 더 다가갈 수 있을 것으로 사료된다.

중심어: 페쇄형 스월 분사기, 유동 불안정, 분사기 자체 불안정, 인젝터 동역학, 기계식 가진기, Kelvin-Helmholtz 불안정

학 번: 2014-21891